

# Development of a seismic source model for probabilistic seismic hazard assessment of nuclear power plant sites in Switzerland: the view from PEGASOS Expert Group 4 (EG1d)

STEFAN WIEMER<sup>1,\*</sup>, MARIANO GARCÍA-FERNÁNDEZ<sup>2</sup> & JEAN-PIERRE BURG<sup>3</sup>

*Key words:* PEGASOS, Switzerland, probabilistic seismic hazard, seismic source model

## ABSTRACT

We present a seismogenic source model for site-specific probabilistic seismic hazard assessment at the sites of Swiss nuclear power plants. Our model is one of four developed in the framework of the PEGASOS project; it contains a logic tree with nine levels of decision-making. The two primary sources of input used in the areal zonation developed by us are the historical and instrumental seismicity record and large-scale geological/rheological units. From this, we develop a zonation of six macrozones, refined in a series of seven decision steps up to a maximum of 13 zones. Within zones, activity rates are either assumed homogeneous or smoothed using a Gaussian kernel with width

of 5 or 15 km. To estimate recurrence rate, we assume a double truncated Gutenberg-Richter law, and consider five models of recurrence parameters with different degrees of freedom. Models are weighted in the logic tree using a weighted Akaike score. The maximum magnitude is estimated following the EPRI approach. We perform extensive sensitivity analyses in rate and hazard space in order to assess the role of declustering, the completeness model, quarry contamination, border properties, stationarity, regional b-value and magnitude-dependent hypocentral depth.

## Introduction

We document one out of four seismogenic source models to be used by the PEGASOS project (Probabilistische Erdbeben-Gefährdungs-Analyse für KKW-Stand-Orte in der Schweiz) (NAGRA 2004) for site-specific probabilistic seismic hazard analysis at the Swiss nuclear power plant sites. The framework of this work is described in Coppersmith et al. (2008), along with a comparison of our model with the other three groups, described in Schmid & Slejko (2008), Burkhard & Gruenthal (2008) and Musson et al. (2008). The location of the sites and an overview of the regional seismicity is shown in Figure 1. Working on a probabilistic seismic hazard assessment (PSHA) within a SSHAC Level 4 study (Budnitz et al. 1997) was a new and rewarding experience for our expert group of two seismologists (Wiemer & Garcia) and one geologist (Burg). The resources provided to us by the project, and the duration of the project of more than 18 months, made it possible for the team to develop a highly detailed model, with some innovative aspects and an extensive representation of uncertainty. We were able to explore the sensitivity of the hazard to some key issues, such as the

role of the completeness model or the declustering procedure, something that in many hazard studies cannot be performed due to the lack of resources. We hope to give subsequent hazard studies in Switzerland and other countries valuable input by making available our model, and the thought process that went into its creation. However, in our opinion the greatest value of the source studies of the PEGASOS project lies in the fact that four groups of experts independently evaluated the same region. By comparing their approaches, much can be learned about the representation of uncertainty in hazard studies.

Our team (EG1d) also takes into consideration the requirement that all views expressed in the technical community should be presented and balanced within the model (Coppersmith et al. 2008). However, while trying to weight alternative interpretations according to their scientific robustness, these interpretations and the weight given to them inevitably reflect our own judgment. We tried to discuss in sufficient detail all relevant issues, such that our thought processes are transparent to the reader. We pay particular attention to the treatment of uncertainties. This publication on its own, however, cannot fulfil the scientific standard of reproducibility, since the resulting

<sup>1</sup> Institute of Geophysics, ETH Zurich, Sonnegstrasse 5, CH-8092, Zurich, Switzerland. E-mail: stefan@sed.ethz.ch

<sup>2</sup> Spanish Council for Scientific Research, Museum of Natural History, Dept. of Volcanology & Geophysics. Jose Gutierrez Abascal, 2, E-28006 Madrid, Spain. E-mail: mgarcia@mncn.csic.es

<sup>3</sup> Institute of Geology, Sonnegstrasse 5, ETH Zurich, CH-8092 Zürich, Switzerland. E-mail: jean-pierre.burg@erdw.ethz.ch

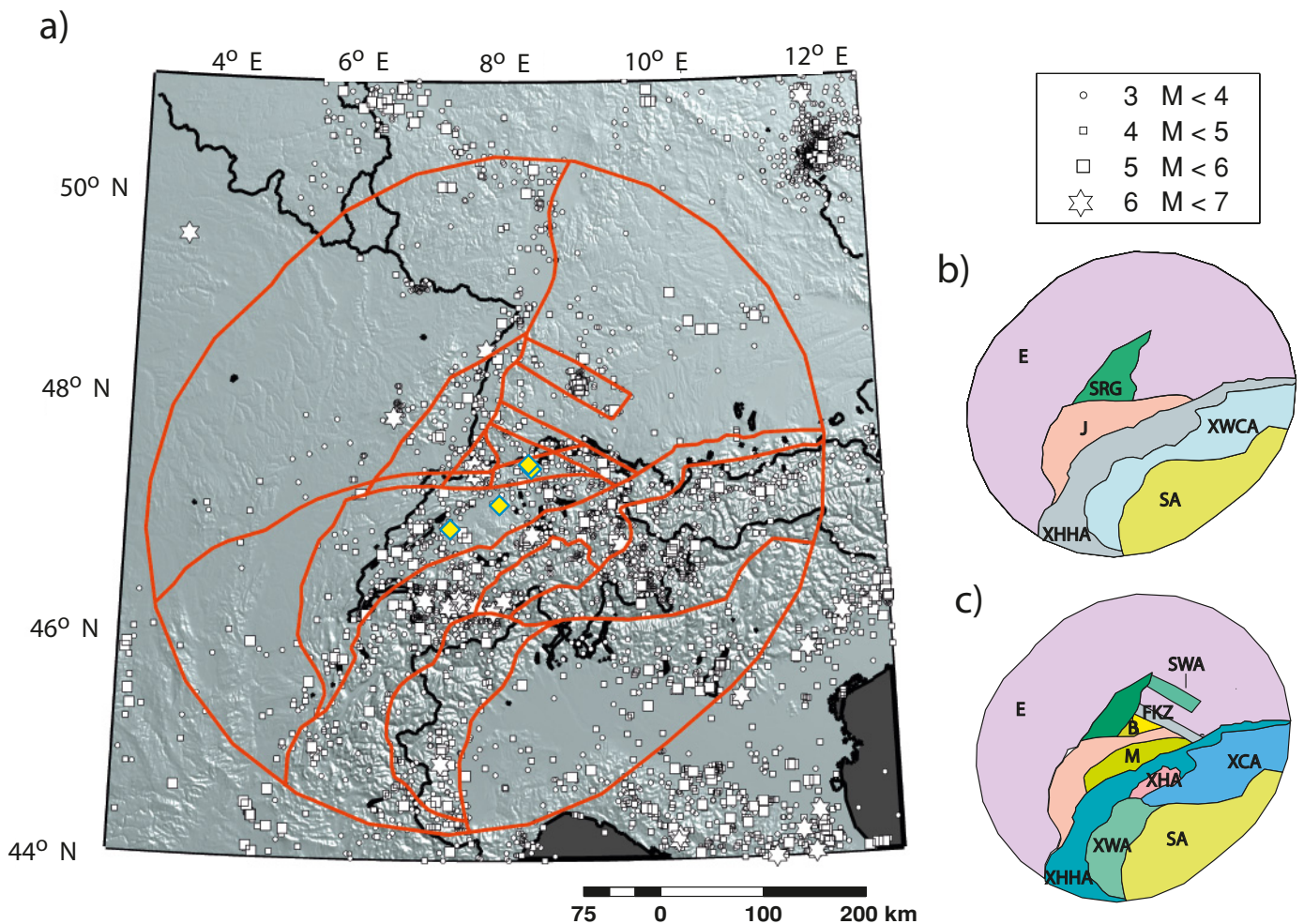


Fig. 1. a) Map of the study region, epicenters of instrumental and historical earthquakes are marked according to their magnitude. Yellow diamonds mark the location of the nuclear power plants for which site specific PSHA is computed in the PEGASOS. The red lines mark one example of seismicogenic areal source model developed in this study. b) Schematic representation of the most basic areal source model of Eg1.d. Labels refer to the codes used throughout the text for the various zones. c) A more refined zonation model.

model has many logic tree branches and rate estimations that cannot be presented here. The full model, however, is available on request through the PEGASOS project (NAGRA 2004).

### Classification of available data

We initially evaluated and prioritised the available information with respect to their usefulness for source zonation in the framework of the PEGASOS project. We implemented the following data classification scheme:

- A) Most Useful. Immediately leads to specific source zones.
- B) Moderately Useful. Can aid in designing source zones, and for consistency check of the zoning.
- C) Marginally Useful. Has little to no-value for source zonation in the framework of the PEGASOS project.

Table 1 summarizes our classification of the available information. From our assessment we conclude that the most important

data source for zonation in the study region are the seismicity record of the past (both instrumental and historical) and the overall geological and rheological units.

### Seismotectonic framework

Switzerland contains several distinct geological and seismotectonic regimes related to the collision of the African and the European plates. In terms of crustal strain rate and seismicity rate Switzerland is located in the transition zone between areas of high seismic activity (Greece, Italy) and areas of low seismic activity (Northern Europe). Small to moderate but persistent seismic activity (Fig. 1) occurs beneath the Alpine belt and north of the Alps, including the Molasse Basin, the Rhine Graben, and the Jura (e.g., Deichmann et al. 2000). The country can be subdivided into three main tectonic units: (1) The Alpine belt in the south, (2) the Jura in the north, and (3) the Molasse basin in between (e.g., Trümpy 1985; Hsü 1995; Pavoni

Table 1. Classification of the available information sources for the usefulness of seismic zonation in the study region. A: Most useful, B: Moderately useful, C: Marginally useful.

Type of information	Class	Remarks
Large-scale geological/rheological units	A	Differences between crustal-scale units are meaningful as they coincide with differences in earthquake depth distribution (transition crystalline Alps – Alpine Foreland) (Deichmann, 1992; Deichmann et al., 2000), differences in the density of earthquakes and differences in isostatic behavior. However, major boundaries between these regions show no signs of recent activation in historical or geological data.
Historical catalog	A	While highly relevant, recurrence times of large events are impossible to establish based on the historical data alone. In areas of moderate seismicity. The uncertainty in magnitude and location is important and most likely large and poorly quantified.
Instrumental seismicity:	A	Important to estimate depth distribution of seismicity, and in order to construct a recurrence model, if combined with the historical catalog. However, it is unclear to what extent the extrapolation from small events to larger ones, and from the most recent times to longer periods, is valid.
Focal mechanism	B	Useful for defining the potential for reactivation of existing faults, for general style of faulting, and to check consistency of zoning. However, it is unclear to what extent we can extrapolation from the observed small events to hazard relevant larger ones. In addition, the available dataset is with only about 170 mechanism sparse.
Paleoseismicity	B	‘Paleoseismic’ events older than 3Myrs are considered to provide no pertinent information for current earthquake hazard. Younger, Holocene evidence is more critical. However, the available paleoseismic evidence (e.g., Meghraoui et al., 2001; Becker et al., 2002) is sparse, fragmented, incomplete, and uncertain in both space and magnitude.
Hot springs	B	Hot springs inform on regions where water circulates deep and fast in the crust and their alignments across lithological boundaries are known to delineate major fracture zones, some of them going down to Moho depth. Their correlation with recent seismic activity is questionable, but such alignments are important for large-scale zoning because they point to crustal fractures, i.e. weak contacts prone to eventual reactivation. Still there is the problem of the interaction between fluids and seismicity, which remains unclear; or at least there is not a direct relationship. In addition, they do not yield a complete set of major fracture zones; other fracture zones, devoid of hot springs and water circulation, may exist.
Vertical movements, geodetic data, strain data	B	Geodetic data help defining broad regional patterns, unless specific and detailed measurements for individual faults exist, which is not the case in Switzerland. Yet, this information indicates seismic potential. In Switzerland and in neighboring areas, rates are homogeneous and overall very low, consistent with GPS measurements. Strain rates are low and do not yield evidence for strain localization at the surface: The average total convergence rate between Africa and Europe for the past 49 Ma is about 0.9 cm/a (Regenauer-Lieb and Petit 1997), which is in good agreement with the rate of 0.94 cm/a for the past 3Myrs, as implied by NUVEL-1 (DeMets et al. 1990). These numbers are reasonably consistent with long-term geological strain rates. Vertical movements are too small to distinguish isostatic due to post-glacial rebound from tectonic signals.
Faults	B	Numerous faults are identified on geological maps at all scales, which reveals an equal potential for earthquakes almost everywhere. In the literature, there is no convincing evidence for Quaternary movements that have offset topography and post-glacial features (e.g. Eckardt et al. 1983). The fact that the Molasse Basin is less faulted than the Jura may indicate that Molasse sediments behave less brittlely than surrounding rock units.
Shallow seismic profile	B	Seismic lines help constraining the deformation ages if no signs of disturbance in the youngest sediments are time significant (thickness 2 sec, about 4 km, several Ma). However, the information available is fragmented and incomplete and might give a statistically biased view. The role of creep versus seismogenic deformation is also unclear. Maps of basin depths are somewhat relevant for zooming, in that they show the distinction of late Paleozoic sediments – distribution of basement and sedimentary rocks. Thin-skin versus thick-skin faulting seems to us not immediately relevant for seismotectonic zonation, because its influence on hazard is not clear.
Paleostress measurements	B	Paleostress measurements have limited value because they are extremely imprecise in direction, shape of stress ellipsoid (hence stress regime) and age significance. In addition, stress fields older than the quaternary are not pertinent to the project purposes. However, fault behaviors documented by paleostress studies were included in the general discussion on style of faulting with respect to stress directions (Homberg et al., 1994; Homberg et al., 1997).
In situ stress measurements	B	Few data available, but reasonably consistent with focal mechanisms. They show that the uppermost continental crust of Switzerland presently is mostly under nearly N–S compression. A broad stress field is consistent across the entire region, including the Rhine Graben, but different regions are dominated by different fault orientations. However, no local information is available for detailed zonation taking into account stress field variations. The lack of local information is limiting the relevance to broad scale zonation and for assessing the potential for reactivation under given stress regime.
Deep seismic profiles, P- and S-wave velocity structure	B	The regional velocity structure may in our assessment identify areas of potential deep activity. From tomographic studies and reflection/refraction seismology, a good knowledge of P-wave velocities down to the Moho exists (Husen et al, 2003). The S-wave velocity structure, however, is largely unknown. In addition, it is not clear how these velocities relate to seismic potential, because ruptures can cut across velocity transients.
Moho depth	C	The Moho surface in the study region is a regional feature that smoothly and regularly deepens southward. To the north of the Alps, it clearly is the bottom boundary of the seismogenic crust. However, it remains unclear how it can be used for zoning since in our assessment, there is no immediate correlation between seismic hazard and Moho depths.
Thickness of the sedimentary cover	C	The vertical distribution of seismic events indicates that the seismic behaviors of the sedimentary cover and the crystalline basement are grossly similar, with the exception of the Molasse basin, which seems to be less seismically active. In itself, the bathymetry of the sedimentary cover appears to have little value.
Topography	C	While topography in some regions of the world correlates weakly with seismic potential, it does in our assessment not provide a suitable basis for zonation in Switzerland that goes beyond an Alpine-Foreland-Rhinegraben classification.
Potential fields (Gravity, Magnetism)	C	Potential fields provide in our assessment regional, large-scale information. Their relevance for zonation is limited because the link between seismic hazard and potential fields is not clear.

et al. 1997). We now briefly describe our assessment of the seismotectonic framework that provides the guiding principles for our zonation:

**Contemporary tectonic processes.** Switzerland is characterized by localized deformation of brittle rock in the slow convergence zone (rates <10 mm/a) between Europe and Adria. (e.g. Muttoni et al. 2001). We are not in a 'pure' intraplate environment. The observed moderate to low seismicity rates, when compared to seismically much more active plate boundaries, are consistent with the low deformation rate imposed by the tectonic system. This regime has been active for at least 1 Ma, probably 5 Ma or more, and we expect it to be similar for the foreseeable future. A high heat flow (thermal anomaly) underneath the crystalline Alps restricts very probably the seismogenic depth in this region to about 15 km (e.g., Deichmann et al. 2000).

**Tectonic provinces.** Several distinctive geological and rheological units are exposed to a broad regional stress/strain field. For a geological overview, please refer to Schmid & Slejko (2008, this volume). Within these large regions, the seismic potential is, to a first order approximation, homogeneous, and seismicity is diffuse. Localized stress concentrations, fluid interactions, zones of weaknesses etc., then give rise to persistent or temporary clusters of activity. In most cases, the actual geological and geophysical reasons for clusters are unclear, and it is uncertain whether historically observed activity centers will remain stationary.

**Thin- versus thick-skinned structural interpretations.** The concept of thin- versus thick-skinned structural interpretations is fundamentally geometrical and has essentially been applied to foreland fold-and-thrust belts to derive rules of thrusting (e.g. Boyer & Elliott 1982). Fold-and thrust belts are typical of most mountain belts and reflect shortening of the upper crust. However, deformation may involve basement (thick-skinned), or be limited to the sedimentary cover, which is detached from the basement (thin-skinned). In the Alps, the discussion has some importance concerning the bulk development of frontal zones such as the Jura Mountains, in which most of the deformation might be localized along a basal décollement, and in the post-Triassic sedimentary cover where thrust sheets deform internally by folding (e.g. Sommaruga 1999). The thin- versus thick-skin interpretation has consequences on the interpretation of the bulk shortening in Miocene to Pliocene times. It has less importance regarding the instantaneous, present-time deformation linked to seismicity. Recorded seismicity shows that the seismogenic deformation is equally distributed over the whole thickness of the European crust in the foreland area, and within the upper 15 km of the Alpine hinterland. Nowhere is the seismicity underlining a preferred décollement plane. The geometrical concept is apparently irrelevant to seismogenic interpretations and it seems more reasonable to accept that seismicity in vertical sections reflects, as in map view, distributed seismogenic strain of the brittle crust. The ductile crust, expected to underlay the hinterland, is not seismogenic because it is too

warm, or because strain rates are too slow. The implication for source models is seismogenic homogeneity down to the lower seismogenic level.

**Spatial distribution of seismicity.** The seismicity distribution (and related activity rates) clearly separates two regions: (1) A higher seismic activity and shallow depths of hypocenters are typical for the crystalline zone in the south (Figs. 1 & 2); (2) lower activity rates, with hypocenters down to the Moho discontinuity characterize the Molasse and Jura areas (e.g., Deichmann et al. 2000). Clusters of persistent activity exist within both zones, but these refer to a very short time period covering the last decades only. The Molasse rocks are poor in seismic events, in particular for high magnitudes. This observation fits rheological expectations as weak sediments dominate the bulk material. Conversely, basement faults, such as the Fribourg strike-slip fault, are reactivated and are potential sources. The Fribourg fault is known thanks to its recorded activity over the last few decades (e.g. Deichmann et al. 2000; Kastrup et al. 2007) yet is one structure of many of its sort that are inferred to exist by correlation with basement outcrops, or known to exist thanks to seismic surveys. The implication is that faults like the Fribourg case may begin to be active at any time below the Molasse sediments and the Jura Mountains.

**Usefulness of stresses/strains.** Stress and strain measurements in the study region (e.g. Regenauer-Lieb & Petit 1997) are important because they provide constraints on maximum magnitude and total seismic energy release over the region. However, because of low strain rates, which are near the resolution limit of modern GPS based campaign, stress and strain measurements provide little insight into recurrence intervals or energy release of individual faults or fault zones. This is a major difference to active plate boundaries, where strain based models can provide important constraints on seismic hazard.

**Assessment of reactivation of existing structures.** Major fault boundaries are candidates for reactivation, depending on their orientation to the general stress field and /or to local stress regimes. This point is highly relevant since e.g. the Fribourg strike-slip fault demonstrates reactivation of old basement fractures (Deichmann et al. 2000; Kastrup et al. 2007). Reactivation potential concerns therefore any basement fault, and in particular the major transcurrent fault zones that bound Permo-Carboniferous trough identified from geophysical surveys below the Molasse basin (Neuchâtel, Northern Switzerland). It also concerns major faults that formed during the Alpine orogeny and Cenozoic extension responsible for both the Rhine and the Bresse Graben on the European lithosphere (e.g. Dèzes et al. 2004; Schumacher 2002).

## Principles of zonation

**Areal sources or line sources.** In our assessment, there is no convincing evidence for active faults and no slip rates on known

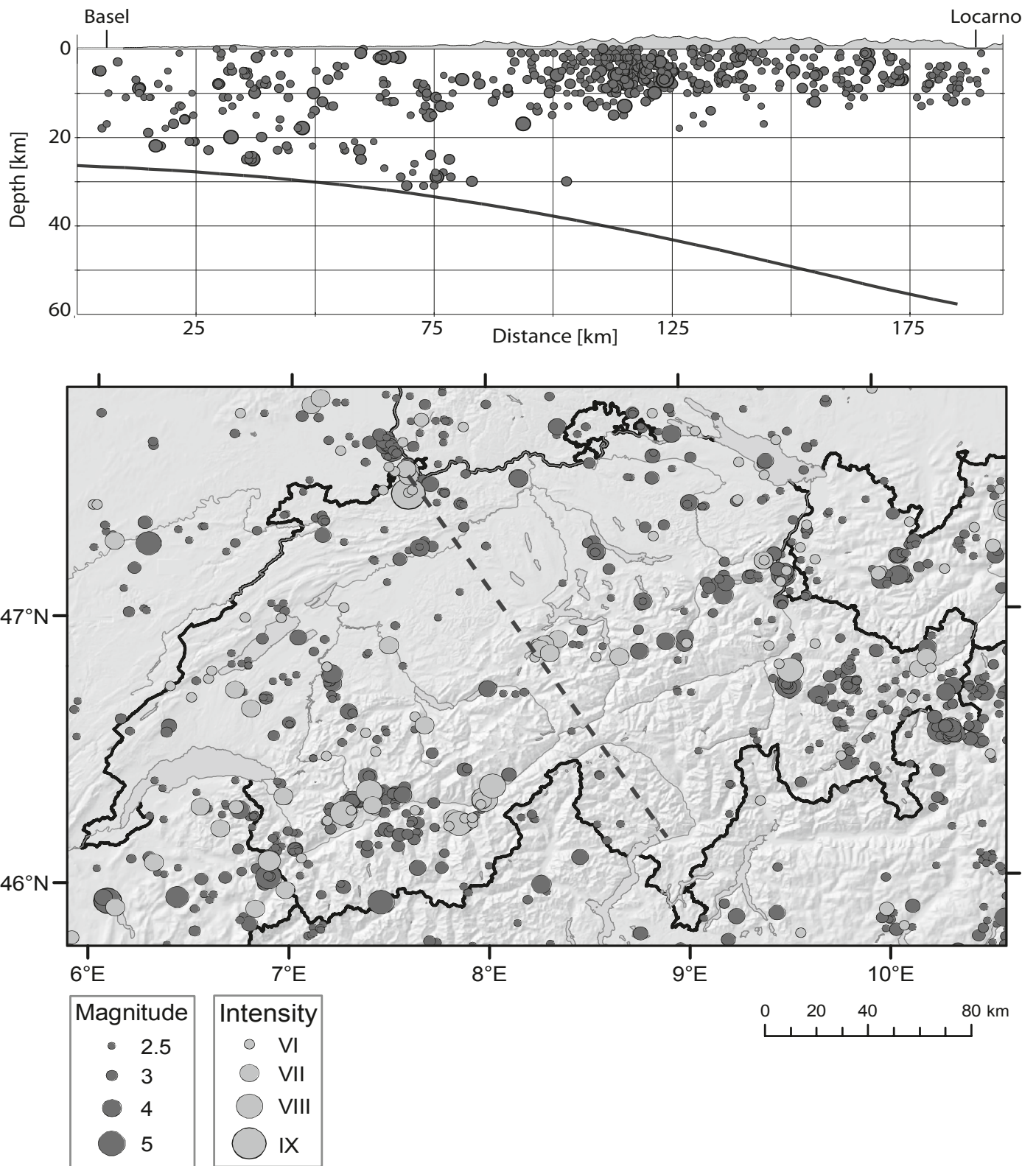


Fig. 2. Bottom frame: Map of the seismicity in Switzerland, dark grey symbols represent instrumentally recorded earthquakes, the size is proportional to the magnitude. The lighter grey circles refer to pre 1975, 'historical' events; the marker size in this case is proportional to EMS intensity. Top frame: Cross-sectional view through Switzerland, approximately following the line Basel – Locarno. Circles mark the projections of hypocenters of well-recorded instrumental seismicity (after Deichmann, 2000).

faults are available in the study region. Consequently, we see no possibility to treat them separately. Major geological/rheological boundaries are not dramatically active faults at current, and may have not been especially active during the last 1–5 Ma. There is no reason to assume preferential activation of these structures in the immediate future. Therefore, areal sources capture best the diffuse nature of the observed, and potential, seismicity in the studied region.

**Stationarity.** The most critical underlying questions for zoning is stationarity, i.e. the degree to which future seismicity will follow the past patterns. We are referring in this context to spatial stationarity, although spatial and temporal stationarity express themselves similarly in seismicity records. This determines largely which zoning strategy should be applied: 1) large regional zones, 2) small source zones, or 3) smoothed seismicity approach (also called ‘historical approach’). We contend that the degree to which stationarity holds in general, and in the study region in particular, is unknown. The applicability of the stationarity approach also depends on the length of the forecast period: For short periods (days to years) stationarity may be more important than for longer periods (millennia+).

**The ‘historical approach’ versus areal zonation.** The ‘historical approach’ in our use of the term is equivalent to a spatially smoothed seismicity, kernel smoothing, or ‘Frankel method’ (Veneziano et al. 1984; Frankel 1995; Frankel et al. 1997; Woo 1996). However, similar results can be achieved using small areal sources and soft boundaries. The strength of the historical approach is the development of a probabilistic forecast based on an optimal statistical representation of the past seismicity, in an objective and reproducible way. Its main weakness is the underlying assumption of stationarity, and the reliance on a complete seismicity record. The strength of the areal zonation based on seismotectonic information (Cornell 1968; Giardini 1999) is the ability to integrate additional geological and geophysical knowledge. Its weaknesses are the possible ambiguity and subjectivity of the interpretations (Frankel 1995), as well as the underlying main hypothesis of seismically homogeneous source zones, i.e. uniform distribution of seismicity.

Both approaches have been widely used in PSHA studies, and are defensible according to our assessment. In our assessment, both should be used in our source modeling as a way to express epistemic uncertainty in PSHA approaches, representing different concepts of stationarity. We integrate these alternative conceptual models regarding spatial stationarity into one model by designing broad source regions based mainly on seismotectonics and subsequently applying variable degrees of smoothing within and across these regions.

**Large-scale versus small-scale zonation.** While it would be desirable to design small zones for higher resolution in hazard, individual zones not solely based on seismicity need to be based on reasonable and defensible assumptions. Smaller scale variations in seismicity are best represented using the historical ap-

proach. Our zonation, therefore, relies mainly on large zones. This expresses our interpretation that in a setting of diffuse seismicity such as Switzerland, seismic potential over broad regions is comparable, and that fluctuations seen in earthquake density within zones may be a temporary fluctuation with limited predictive value.

**Source boundary properties and their meaning.** We prefer to define boundaries that have more than one justification derived from the geological, rheological, geophysical (field gradients) or a seismicity record. As such, the zone boundaries delineate major contacts that can be identified in any geological map. The dip of such major boundaries has uncertainties that bear some importance in the boundary regions.

**Characterization of faults versus zones.** Avoiding bias due to the use of known active faults was further motivation for large “predictive” zones. In our opinion, there is no convincingly demonstrated geomorphology that can be linked to any specific fault activity younger than the last glaciation event (with the disputable exception of the Reinach fault), mostly because fractures associated with soil creeping or instability on steep mountain slopes can mimic fault traces. Consequently, none of the faults reported on geological maps and in the literature can be considered as potentially more seismogenic than the others. In the case of the Reinach Fault, recent work (Meghraoui et al. 2001) has drawn much attention that over-amplifies its real importance as a potential source, because several other recent faults mapped in the Basel area may also be the actual source of the 1356 Basel earthquake. Uncertainties in terms of location in both map view and depth do not allow identifying the actual location of this historical event.

**Energy conservation.** The summed moment release over the historic record, which is consistent with the observed geological strain rates in the study region, needs to be conserved over time.

**Faulting styles.** Faulting style includes relative movements along fault planes along with the predicted orientation of ruptures within each areal source zone. Therefore, faulting style should take into consideration the regional strain/stress field as well as its local perturbations. Focal mechanisms provide instantaneous information; yet, they do not give access to the integrated bulk pattern. This discrepancy in time scale on several mechanisms governing strain, thus seismogenic deformation, leaves open a broad uncertainty concerning faulting style. Concerning relative movements, the faulting style is simplified to three end members, i.e. thrusting, strike-slip and normal faulting. The three of them accommodate strain and may be coeval, depending on the fracture orientation, and may combine. Concerning the predicted orientation of ruptures, we assume that the local state of stress will tend to reactivate existing faults, or create new ones, in accordance with the Mohr-Coulomb criterion. In this case, the acute angle between conjugate faults is

bisected by the greatest principal stress  $\sigma_1$ . The Mohr-Coulomb criterion implies that the yield envelope is a line of slope  $\tan \phi$ , with  $\phi$  the angle of internal friction, then the angle between  $\sigma_1$  and each fault plane is  $45^\circ - (\phi/2)$ . Of paramount importance is the orientation of the greatest principal stress  $\sigma_1$ . Therefore, our assessment takes into consideration the focal mechanisms along with the dominant fault pattern reported in each area. Table 2 offers the detailed assessment of the faulting styles in the source zones designed in our model.

### Areal source zone design

Figure 1b shows the few large-scale tectonic zones that are the baseline of our assessment. We refine this simplest starting model in seven decision steps to a more refined model (Fig. 1a & 1c). Below we discuss the reasoning behind the decisions made.

#### Major source zones

##### 1) Helvetic Front: Alpine Foreland and Alps proper

The Helvetic Front is a major crustal boundary that separates two distinctly different source zone environments. The major separation between the Alpine Foreland and the Alps proper is based on: (1) depth distribution of the events (Deichmann 1992; Deichmann et al. 2000), (2) geological information (geological maps of Switzerland) and (3) density of the seismic events. This boundary, the Helvetic Front, is readily seen on any geological map with different rock units to the south and to the north, i.e. lithologies with different rheological/mechanical properties. The tectonic contact zone dips towards the south at an angle of 30 to 45°. A broad thermal anomaly (Jaboyedoff & Pastorelli 2003, and references herein) may limit the depth distribution of the seismic events since the seismogenic (brittle) crust is constrained to be about 20 km thick underneath the Alps, in contrast to the >30 km seismogenic thickness to the north. The seismic activity along the Helvetic Front is apparently contained within the Alps proper rather than in the Foreland.

Because the seismogenic depth differs north and south of the Helvetic Front, two separate depth profiles are used. For computing the depth distribution, we used a relocated dataset of high quality hypocenters, provided by Husen et al. (2003). The corresponding depth distributions are listed in Table 3. Because the Helvetic front is quite far from the sites of interest, we decided to represent it as a vertical boundary rather than an interface dipping 30° S down to 30 km, the depth of the Moho surface documented in the region.

##### 2) Insubric line separating the Southern Alps from the Crystalline Alps

The Insubric (also called peri-Adriatic) lineament is a long-known fundamental tectonic boundary in the Alps. A wealth of data provides several lines of evidence for different crustal

Table 2. Distribution of the faulting styles for the different area sources.

Source Zone	Strike slip [%]	Normal [%]	Thrust [%]
Europe (NEW, SWA, FKZ, TZ)	85	5	10
Southern Rhine Graben	75	20	5
Northern Rhine Graben	85	10	5
Jura (J)	75	5	20
Italy (SA)	70	10	20
Alps (SA, XWCA, XHHA, HA, XHA, XCA, XWA)	70	15	15

characteristics on both sides of this fault: The Insubric line separates the crystalline Alps, to the north, from the Southern Alps, to the south. The Southern Alps were built on the Adria (Italy) microplate whereas the crystalline Alps derive from continental fragments that either belonged to the southern margin of Europe, or were isolated within the Tethys Ocean before collision between Adria and Europe (e.g. Schmid & Kissling 2000). The following geophysical information confirms geological differences: reflection seismology (Kissling 1993; Schmid et al. 1997; Ye et al. 1995), seismic behavior (less active towards the south), gravimetric data and Moho depth. The Insubric Line is a nearly vertical and sharp contact. In our model it is the second major crustal boundary that separates two distinctly different source zone environments. It borders the following source zones: SA (Southern Alps); XWA (Crystalline Western Alps); XCA (Crystalline Central Alps); XHA (Crystalline Helvetic Alps).

##### 3) Penninic Front separating the Crystalline Alps (XWA, XCA sources) and the Helvetic Alps (HA, XHA sources)

Geological maps show the Penninic Front as a major thrust placing the northern parts of the crystalline Alps over sediment-dominated allochthonous units (the Helvetic Alps). Crystalline and sedimentary rocks have marked rheological and behavior

Table 3. Percentiles of earthquakes as a function of depth north and south of the Helvetic Front.

Depth Range [km]	North of HF [%]	South of HF [%]
0– 4.99	12.50	44.48
5– 9.99	23.91	47.00
10–14.99	27.17	8.02
15–19.99	14.67	0.38
20–24.99	13.58	0.1
25–29.99	5.43	0
30–34.99	1.08	0
35–39.99	1.08	0
40–44.99	0.54	0
45–49.99	0	0

Table 4. Magnitude of complete reporting,  $M_c$ , for different regions. For each region, two completeness estimates were derived.

Period	Model 1 [Mw]	Model 2 [Mw]
<i>Switzerland</i>		
1300–1600	6.0	6.0
1600–1750	5.5	5.7
1750–1880	4.7	5.0
1880–1977	3.0	4.2
1977–2001	1.8	1.9
<i>Italy</i>		
1775–1880	5.5	5.7
1880–1979	4.1	4.3
1979–2001	3.2	3.2
<i>Austria</i>		
1700–1896	5.5	6
1896–1978	3.1	3.3
1978–2001	2.5	2.5
<i>France</i>		
1700–1880	5.3	5.3
1880–1978	3.7	4.0
1978–2001	2.2	2.2
<i>Germany</i>		
1300–1620	6.0	6.5
1620–1870	5.4	5.6
1870–1980	3.1	3.5
1980–2001	3.0	3.1

differences and their mapped occurrences point to the presence of pieces of upper crust with different bulk composition and behavior on both sides of the Penninic Front. Based on geological information and seismic reflection profiles this separation is well constrained as a south-dipping contact  $30 \pm 10$  km, which is supported from seismic evidence, and somewhat supported by stress directions. The pre-instrumental activity in the Wallis region may in our assessment possibly belong to the Helvetic Alps. The same is true for the St.Gallen-Rheintal activity, because of the dip of the structure. While we discussed to treat this boundary as a 3D structure, we ultimately decided to not do so given its distance from the sites, and the aforementioned alternative mechanisms to express boundary uncertainty. We considered four alternative interpretations:

- *The Simplon Fault subdividing XWA and XCA.* The Simplon fault is described as a major normal fault that was active until about 5 my ago (Mancktelow 1985). This major fault does separate two regions, but its structural reality seems to have no expression in Quaternary tectonics. Fur-

thermore, it does not mark any major separation between distinct seismogenic regions. On the one hand there is a major, crustal-scale tectonic contact; on the other hand, there is no evidence for its recent and present day reactivation. Therefore, we consider a single Crystalline Alps source area as equally likely as a divided one, and we thus treat them as two equally weighted branches in the logic tree (50% to 50%).

- *Separation between the XHA and HA.* The seismic distribution suggests the possibility of such a separation. However, lithologies and the general deformation and metamorphic history of both zones are the same. There is no clear-cut geological explanation for this anomaly in seismic distribution. This alternative is therefore an unlikely scenario that is treated as a logic tree branch with small weight (10% probability).
- *Subdividing the Valais activity:* We feel that the evidence for clustering is purely seismological: It is therefore best taken care by a ‘historical approach’.
- *Engadine fault as a source fault.* We contend that there is currently no decisive geological evidence, only seismicity (historical: observed effects in the valley). Also, the faults would be far from the sites and hence of little interest.

#### 4) Jura (J source)

The Jura source zone is separated from other sources on the basis of rock composition and the existence of a shallow-dipping contact zone between the deformed sedimentary cover and the apparently less deformed basement (pre-Triassic rocks), i.e., ‘décollement’ (e.g. Burkhard 1990, Sommaruga 1999). We decided to put vertical boundaries to the N and W because they are reported to be subvertical strike-slip (for the N) and normal (for the W) faults (Truffert et al. 1990). Individualizing this zone expresses the different activity rates of the Jura when compared to Europe (E source). However, this difference in strain and seismicity refers mostly to the near-surface of the Jura Mountains, which comes at variance to the Molasse basin for which the near surface is nearly silent. The boundary between Jura and Molasse (M source) attempts to express in 3D this seismogenic difference. To the northeast, the border of the Molasse basin has no significance to zoning: It is stopped at Bodensee, where a NW–SE late-Paleozoic strike-slip fault runs against the Helvetic Front. The Molasse could be modeled as a 3D wedge with  $M_{max}$  of 4.0. However, we feel that the Molasse source does not need separate treatment because the weighted magnitude-dependent depth distribution produces a zone at the surface  $\sim 2$  km thick in which no hypocenters occur.

#### 5) Southern Rhine Graben (SRG source)

To express the Rhine Graben activity we first define a wide north-south trending zone that includes the Rhine Graben and its shoulders. This zone was then subsequently divided into a northern and a southern part along the Variscan suture zone,

the Lalaye-Lubine Fault in the Vosges to Baden-Baden in the Black-Forest, the Erstein Sill below the sedimentary infill of the Rhine Graben (Villemin et al. 1986; Sissingh 1998). This across-graben division is consistent with different temperature and composition characteristics of observed hot springs, and with the thermal anomalies. We also consider the possibility that the northern part of the graben is an independent source, NRG. To express these alternatives, we treat the existence of the NRG source as a logic tree branch with a 50% weight. If it does not exist in the model, the area north of the suture zone is integrated into the Europe Zone (E source). We considered four alternative interpretations:

- *Specific sub-zone around Basel* (B source) separated from the remainder of the SRG source. The Basel region has experienced the largest earthquake in the study region in historical times, a magnitude 6.5 or larger event in 1356. Paleoseismic studies (Meghraoui et al. 2001) suggest that similar size events have taken place on the Reinach fault. There is evidence for at least three earthquakes, which occurred on that branch of the fault within the last 8500 years with vertical displacements ranging from 0.5 m to 0.8 m. To incorporate the special nature of the Reinach region into our model, we construct a small source zone that incorporates the Reinach fault. On the other hand, in our assessment is also possible that events such as 1356 can occur anywhere within the SRG source. Therefore, we treat the Basel source as a logic tree branch with a 50% weight. In addition, we note that by later on explicitly addressing the epicenter uncertainty, the 1356 Basel event will be probabilistically distributed over neighboring source zones.
- *Southern Rhine Graben Transfer Zone* (TZ source) The Southern Rhine Graben Transfer Zone (Niviere & Winter 2000) is a Northern-Jura border active fault system zone. This fault zone is geologically known to be an important fault zone that probably initiated during the Carboniferous (e.g. Arthaud & Matte 1975), was reactivated throughout the Mesozoic and in the Tertiary as a transfer between the Rhine and Bresse Grabens (Villemin et al. 1986; Sissingh 2001). This fault zone has the potential to be reactivated under the current stress regime, consistent with focal mechanisms and differences in geodetic uplift behavior. According to there is a small probability that the 1356 Basel event in fact took place along this structure. To address this potential that the TZ is active or reactivated, we incorporate it as a separate source area, but with a small weight of 0.05.

#### 6) Europe (E source)

The source zone encompasses combined North-Eastern and North-Western Europe plus the northern part of the Rhine Graben north of SRG up to about 50°N (inside the limits of the 300 km circles around the investigation sites). Geological knowledge in this zone is generally more limited, because of lack of geological information in flat areas. Seismicity in the E

source is generally low and diffuse in nature, with no specific centers of activity besides those ones discussed below.

#### *Additional and alternative zones*

**Bresse Graben.** The Bresse Graben is one of the Tertiary extensional basins that formed within Europe (e.g. Sissingh 1998, 2001; Ziegler 1992). It bounds the Jura Zone, to the West and stops, to the North, against the TZ Permo-Carboniferous trough that was reactivated during the Tertiary as a transfer zone between the Bresse and the Rhine Grabens. Although it is geologically related to the Rhine Graben, we did not find it pertinent to define a separate zone, as we do not individualize the Northern Rhine Graben in the basic zone model either. This decision refers to both geological and seismological information (Truffert et al. 1990; Grellet et al. 1993). From a geological-structural point of view, the Bresse Graben expresses an amount of extension significantly smaller than that in the Rhine Graben; the Tertiary volcanism, voluminous in places of the Rhine Graben, is absent in the Bresse Graben. Absence of volcanism emphasizes the difference in lithospheric history. Therefore, the Bresse Graben cannot be treated on the same level as the Rhine Graben. The Bresse Graben is only the northern segment of the Rhone – Golfe du Lyons extensional system that produced eastward drift of the Corsica-Sardinia Block from the Iberian Peninsula. The extensional deformation that could have differentiated the Bresse Basin from Europe concentrated in the new oceanic basin, leaving quickly the Bresse Graben as a part of continental Europe. Not surprisingly, the seismicity distribution does not display any difference in behavior between the Bresse Graben and adjacent parts of Europe. The distribution of other features such as hot springs (PEGASOS unpublished document) shows that there is less difference between the Bresse Graben and the bulk of Europe than between the latter and the Northern Rhine Graben. Flat lying and unfaulted Quaternary infill sediments suggest that seismicity possibly occurring in this structure would preferably take place on the main boundary faults limiting the Jura Zone to the east, and the long, westward continuation of the Permo-Carboniferous trough to the North. Such seismogenic events can thus be integrated in the neighboring zones, giving less ground to make a very low probability, specific Bresse Graben Zone. In summary, the Bresse Graben does not deserve a special treatment with respect to the bulk Europe (E source).

**Freiburg Konstanz zone (includes Freiburg – Bonndorf – Bodensee Graben)** (FKZ source). The Freiburg Konstanz zone is inherited from Permian Carboniferous tectonics as a conjugate fault zone in respect to the TZ zone (Arthaud & Matte 1975). Its WNW–ESE strike has potential for reactivation under the present-day stress field and aligned hot springs show that this fracture zone may extend relatively deep into the crust. It is also visible from geodetic differences in uplift rates (PEGASOS unpublished document). However, there is no clear sign of current seismic activity. We decided to incorpo-

rate the possibility of re-activation of the FKZ as a logic tree branch, but with a very low probability (weight: 0.05).

**Swaebian Alb** (SWA source). The Swaebian Alb is a documented zone of episodic activity with consistent strike-slip focal mechanism, propagating in a NS direction. In our model, the clustered activity is incorporated through the spatially smoothed model, which adequately expresses the current activity but also allows for migration of this activity, depending on the degree of stationarity. Despite the NS orientation of the recorded activity zone, we take into account there is a small probability that the active zone is not simply a Riedel direction highlighting the potential for localized activation of a larger, NW–SE trending zone, parallel to the FKZ. To address this possibility, which in itself is not adequately represented by smoothed seismicity, we define the SWA zone with a low weight of 10%.

The simplest starting model is composed of six sources (Figure 1b) i.e. E, SRGB (SRG + B), J, XHHA (HA + XHA), XWCA (XWA + XCA), and SA. The alternative models obtained from the seven decision steps carried out are summarized in Figure 1c:

### Maximum earthquake magnitude

Maximum magnitude (hereafter  $M_{max}$ ) is generally recognized as a critical parameter with considerable influence on the final hazard for low probability assessments. It is also the parameter most difficult to assess in the study area, because the physical understanding of  $M_{max}$  is limited, and the database to derive this parameter is statistically very limited. Therefore, most importantly,  $M_{max}$  has to be specified with a broad uncertainty.

We evaluated several techniques used in past evaluations of  $M_{max}$ , ranked below in order of descending significance in our opinion, although none of them provides a satisfying answer to the problem:

1) **The EPRI approach based on a global database** (Johnston et al. 1994): Although, as stated below, none of the available methods provides a satisfying answer to the  $M_{max}$  problem in the PEGASOS area, we favor the EPRI approach (Johnston et al. 1994) for the estimation of  $M_{max}$  as the most satisfying compromise option. Specifically, we appreciate the broad uncertainty distribution of  $M_{max}$ . We consider the prior distribution for extended continental crust, with a mean magnitude of 6.4 and a standard deviation of 0.84) appropriate for the study region, because extension dominated the European crust in Permo-Carboniferous times (e.g. Burg et al. 1994), during the Mesozoic development of the Tethys passive margin (e.g. Ricou 1994) and during Tertiary extension (e.g. Ziegler 1992), and because the broader uncertainty distribution of extended crust expresses more accurately the notion that  $M_{max}$  is uncertain. Following the EPRI approach,  $M_{max}$  will be modified in each source zone to reflect the recorded seismicity.

- 2) **Strain and displacement data constraints** (Regenauer-Lieb & Petit 1997; DeMets et al. 1990). The lack of geological evidence for active faults larger than 30 km (capable of events of roughly  $M6.5$ ) is consistent with a back of the envelope strain rate consideration we explored as a sanity check on the input model. We can convert the seismic moments of the past 700 years into average annual strain, using a Kostrov model (Kostrov 1974). The main free parameters of such an analysis are the geometry of the deformation source region and its depth extent. Using 15 and 30 km depth extent, and a polygon that includes the region of the highest moment release (Basel) we computed values of shortening rates between 1.0 and 0.5 mm/year, respectively. These values are consistent with the deformation rates inferred for the past 3 Ma. In a second step, we can explore which displacement rates would result from an assumed  $M_{max}$ , given a historically observed a-value (1.82) and b-value (0.75) for the same region, assuming a truncated Gutenberg-Richter model. We find that a 1 mm/year strain rate is compatible with a truncated Gutenberg-Richter model with an assumed  $M_{max}$  of about 6.5. If  $M_{max}$  is assumed to be 8.0, however, the required average deformation rate would be about 10 mm/year, which is not witnessed in the geological record of recent GPS surveys. While this rough strain rate analysis has many uncertainties, it suggests that  $M_{max}$  values much larger than 7 are not compatible with the known geodetic record.
- 3) **Global statistical models** (Kagan 1999; Kagan & Jackson 2000). Some purely statistical studies of  $M_{max}$  have been based on global instrumental datasets (Kagan 1999; Kagan & Jackson 2000). These studies suggest that there is little evidence to assume regional variations of  $M_{max}$ .
- 4) **Seismotectonic constraints (Maximum available feature)** (Wells & Coppersmith 1994). Maximum available structure length (Wells & Coppersmith 1994) can be a powerful criterion, although it has been challenged in its usefulness as a predictive tool (D.D. Jackson, personal communication, 2002). The main obstacle to applying it in Switzerland is that we have some disputed and mostly no information on active faults in the region. Even for the Basel region, excavation of the Reinach fault offers little beyond the insight that the event had a magnitude of  $6.5 \pm 0.5$ . It remains unclear whether the Reinach fault, for example, could in rare instances rupture much further along the Rhinegraben, resulting in a much larger earthquake. We retain that there is no identified active fault with rupture longer than about 30 km.
- 5) **Kijko numerical approach** (Kijko & Graham 1998; Kijko et al. 2001). This approach to assess  $M_{max}$  based on recorded seismicity includes a non-parametric estimation that avoids any specific frequency-magnitude distribution. It seems to be a robust technique when applied to complete catalogues that span at least one seismic cycle. However, it has according to our assessment significant limitations in areas of low to moderate seismicity. For that reason, we do not consider its application in this study.

6) **‘One step beyond’ method** (e.g. Slejko et al. 1998). The ‘one step beyond’ technique that was for example employed in Italy, does not seem appropriate for this study, because we are explicitly interested in low probability levels as we are in a region with a low strain rate. Therefore, the seismicity record of about 1000 years within the region does not offer sufficient insight into the maximum possible earthquake.

While we feel that the EPRI approach is best suited to capture the uncertainty in  $M_{max}$ , we also need to make a decision about the upper truncation boundary. EPRI’s prior is, in theory, unbound; yet it is unavoidable to limit it, because otherwise energy is not conserved. Moreover, magnitudes beyond  $M8$  are by most earth scientist not considered possible outside of active subduction zones, because they have not been observed and because the necessary faults with lengths of more than 200 km are not available. Since we are also far away from subduction zones, where  $M8+$  events could originate, and because  $M8+$  events are inconsistent with the aforementioned available deformation and strain rate information, we make the decision of truncating the EPRI distribution at  $M8.0$ .

Large earthquakes of  $M7.5 - M8.0$  are on the other hand in some interpretations (e.g. statistical studies by Kagan and Jackson; i.e. Kagan 1999; Kagan & Jackson 2000) theoretically possible in all seismogenic regions, although with very low rates. Events of magnitude  $M7.5-8$  have occurred within the stable continental crust for example the New Madrid (USA) earthquakes. However, in our assessment there is only a smaller probability of such events in the study region, because the European lithosphere of the study area is younger and warmer than that of Eastern North America, and because they have not been observed in the historical or geological record so far. No structures are known to us in the study that could generate an  $M7.5-8$  event. However, to reflect the aforementioned statistical studies and evidence from other regions, and also in order to allow for the possibility that we lack some fundamental knowledge on seismogenic processes in the study regions, we choose to allow for events with  $M7.5$  to  $8$  with a small probability. We therefore develop two alternative branches that both apply EPRI: (1) Truncation at an upper  $M_{max}$  bound of  $M7.5$ ; (2) Truncation at an upper  $M_{max}$  of  $M8.0$ .

We are fully aware that in some cases the  $M_{max}$  in an areal source zone may result in a rupture considerably longer than the length of this source zone. This is accepted because we do not assume that areal source zones have boundaries impermeable to rupture. This notion is embedded in our model when considering spatially smoothed seismicity rather than discrete source zones. Ruptures have been shown to be able to jump large distances (kilometers) from one fault to another, using static and dynamic stresses as the transport mechanism. We could envision such a scenario as one possibility on how ruptures can incorporate rupture in two or more source zones at once.

## Earthquake recurrence relationships, logic tree design and implementation

In this chapter, we define the logic tree that allows for the computation of earthquake recurrence relationships. It also discusses all necessary choices for recurrence rate computation, such as declustering, completeness assessment, treatment of mining activity etc. Results from the sensitivity analysis are also considered. In some cases they lead us to eliminating certain branches of the logic tree. However, we leave such branches in the discussion in order to document our thought processes and to provide guidance for other hazard studies. Our final logic tree consists of nine decision levels. The tree is schematically shown in Figure 3. Below, we discuss each level in detail.

### Level 1: Input data

The ECOS catalogue (Fäh et al. 2003) contains events qualified as ‘questionable’ or even uncertain (Field identifier: *cc*). These events have a small probability of actually having occurred (Fäh, personal communication 2002). Consequently, we consider it inappropriate to use them for rate computation. Our subsequent analysis is based only on events classified in the ECOS database as certain (*cc* = 1). The ECOS catalogue also contains a number of identified explosions (Field identifier: *Type*). Explosions contaminate rate computation and *b*-value estimations and need to be excluded from the analysis. Only events with an identifier of 3 or higher should be used.

Nevertheless, more than 500 unidentified explosions remain in the data set (Wiemer et al. 2008). This is not surprising, because essentially all earthquake catalogues contain unidentified explosion events. Their identification based on waveform studies is extremely time-consuming and still ambiguous events will remain. In order to address the problem of quarries, we opt for a largely statistical identification and removal of events, following the approach proposed by Wiemer & Baer (2000). This removes about 1000 events from the ECOS catalogue. Their magnitudes are relatively small and they are all contained in the last 25 years of data.

Because of the uncertainty in the quarry identification, we treat both catalogues (original and ‘dequarried’) as input to subsequent calculations, forming the first two branches of our logic tree (equal weight). The feedback from sensitivity results (e.g. Fig. 4), however, shows clearly that de-quarrying has an insignificant effect on the hazard at the sites of interest. For the final analysis, we prefer the de-quarried catalog, including the removal of the French quarry region.

### Level 2: Declustering

This branch expresses the epistemic and aleatory uncertainty of different declustering approaches. Declustering is necessary, because the assumption of a stationary Poissonian process made in the subsequent hazard computations is not fulfilled in the original catalogue. It is our conclusion that no unique and

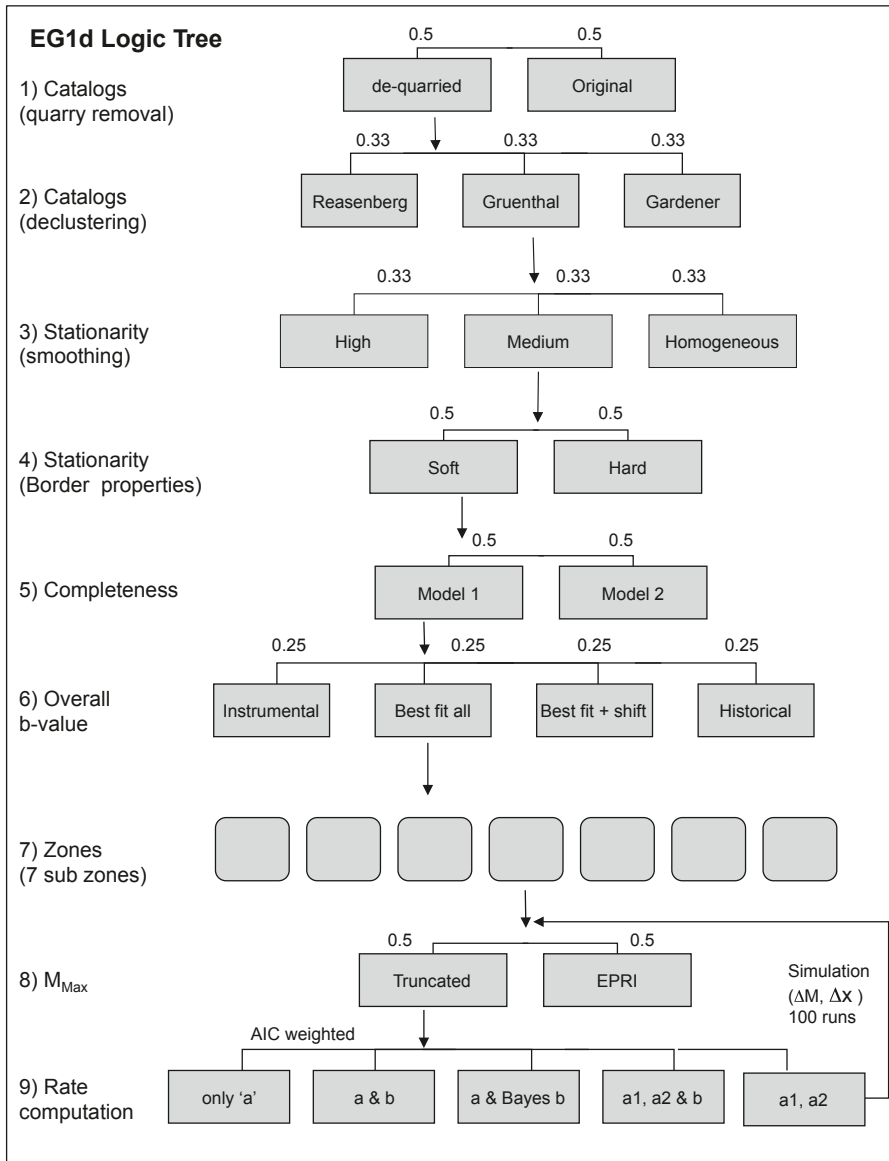


Fig. 3. Logic tree representation of the Eg1d model. Small number next to each branch represent the relative weight.

generally accepted approach to declustering exists. To express the epistemic uncertainty of alternative connectional models of declustering, and alternative approaches to implementing these models, we apply two different methodologies: Reasenberg's physically-based declustering (Reasenberg 1985), and Gardener and Knopoff's (1974) fixed window declustering. To express the aleatory uncertainty in choosing the correct window parameters in Gardener-Knopoff's approach, we allow for two different settings: The original code proposed by Gardener & Knopoff (1974) and the Gruenthal's modified parameters for Central Europe. These algorithms result in considerably different numbers of events in the catalog. It is, however, questionable whether the algorithms have indeed an influence on the resulting rates and b-values for individual zones, or, even less likely, on the  $M_{max}$  estimation.

The sensitivity feedback demonstrated that indeed the effect of the declustering on the final earthquake rate forecast is insignificant (e.g. Fig. 4). Therefore, using only one declustered catalogue is sufficient. We decide to use only Gruenthal's windowing parameters because it is the only algorithm calibrated for the region, including specific evaluations on selected Swiss earthquake sequences (N. Deichmann, personal communications, 2003).

#### Level 3: Stationarity (Smoothing)

This level and the subsequent level 4 both express the uncertainty in the degree of spatial stationarity of seismicity. In our assessment, the degree of stationarity is largely unknown and needs to be expressed as one of the principal uncertainties in

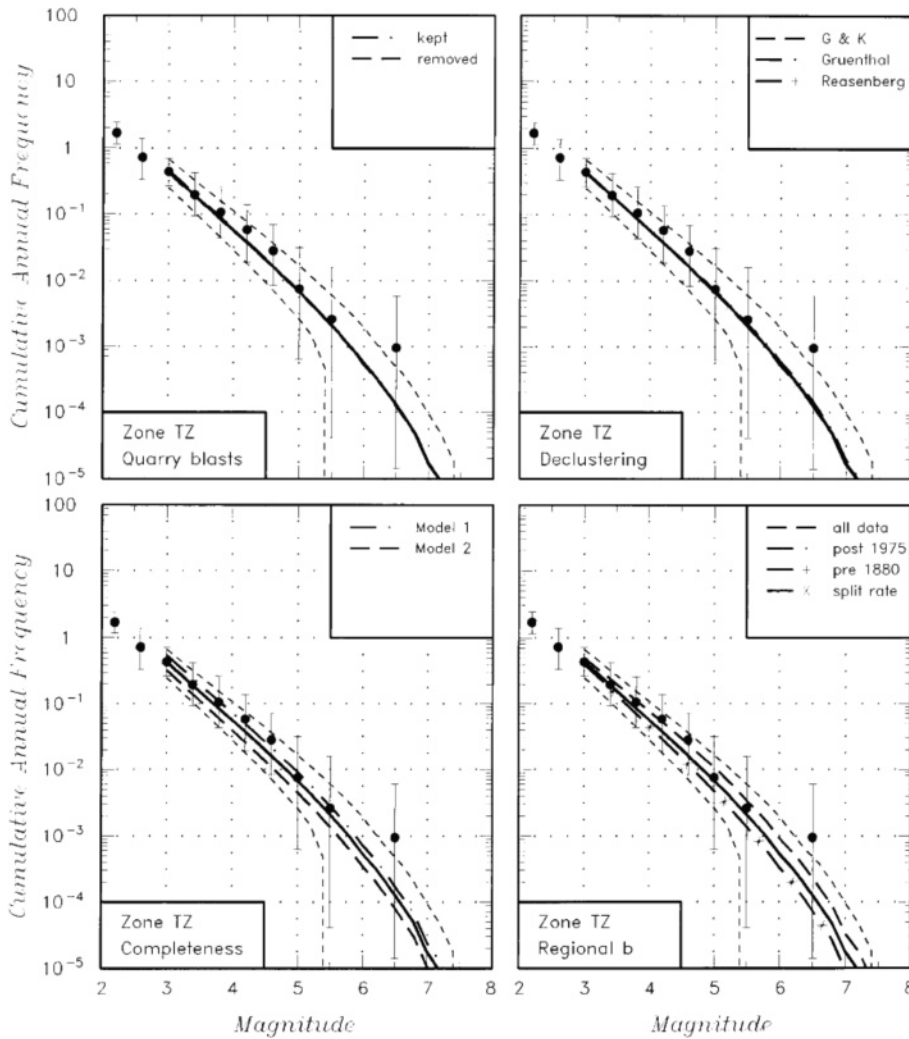


Fig. 4. Sensitivity of the cumulative annual frequency of earthquakes in the model for zone TZ. Upper left: Removal of quarry blasts; upper right: Declustering model; lower left: Completeness model; lower right: regional b-value. Note how quarry blasts removal or declustering do not change the final recurrence rate estimate, whereas completeness model or regional b-value choice does.

the hazard assessment. To represent this uncertainty in stationarity, we apply variable levels of spatial smoothing rates based on the recorded seismicity within seismogenic areal zones. Three levels of smoothing are in our assessment sufficient to express the degrees of stationarity,

- 1) *Homogeneous*: The rate of earthquakes is constant within an areal source region;
- 2) *High*: The rate of earthquakes varies within area sources depending on the density of past earthquakes. The density distribution is obtained using Gaussian kernel smoothing with a kernel width that shows clusters of events to be reproduced.
- 3) *Medium*: The rate of earthquakes varies within area sources depending of the density of past earthquakes. The density distribution is obtained using Gaussian kernel smoothing with a kernel width that shows the larger scale differences between regions to be reproduced.

Each model is represented as a logic tree branch, each receives equal weight. To decide which smoothing kernel represents the three conceptual levels of stationarity best, we evaluate six rate density maps, computed for kernels of 5, 10, 15, 20, 30, and 50 km. Because rate density is a local feature, regional and temporal differences in completeness are not critical in the estimation. We select two kernels to represent high and medium stationarity: 5 and 15 km, respectively. These are shown in Figure 5. From these two maps, a smoothing matrix can be extracted for each zone. This matrix, normalized to one, will then be used to spatially distribute the a-value assigned to each zone. The sensitivity analysis (Fig. 6) confirms that the final hazard is significantly influenced by the smoothing parameter.

Uncertainty in epicentral location is explicitly taken into account in the smoothing. This is accomplished by convolving the location uncertainty into the kernel operator. For a Gaussian kernel,  $h(\text{total}) = \text{sqr}t(h(\text{error})^2 + h(\text{kernel})^2)$ . The uncertainties in epicentral error are given in the ECOS catalog (Fäh et al., 2002). We interpret the uncertainty bounds given in

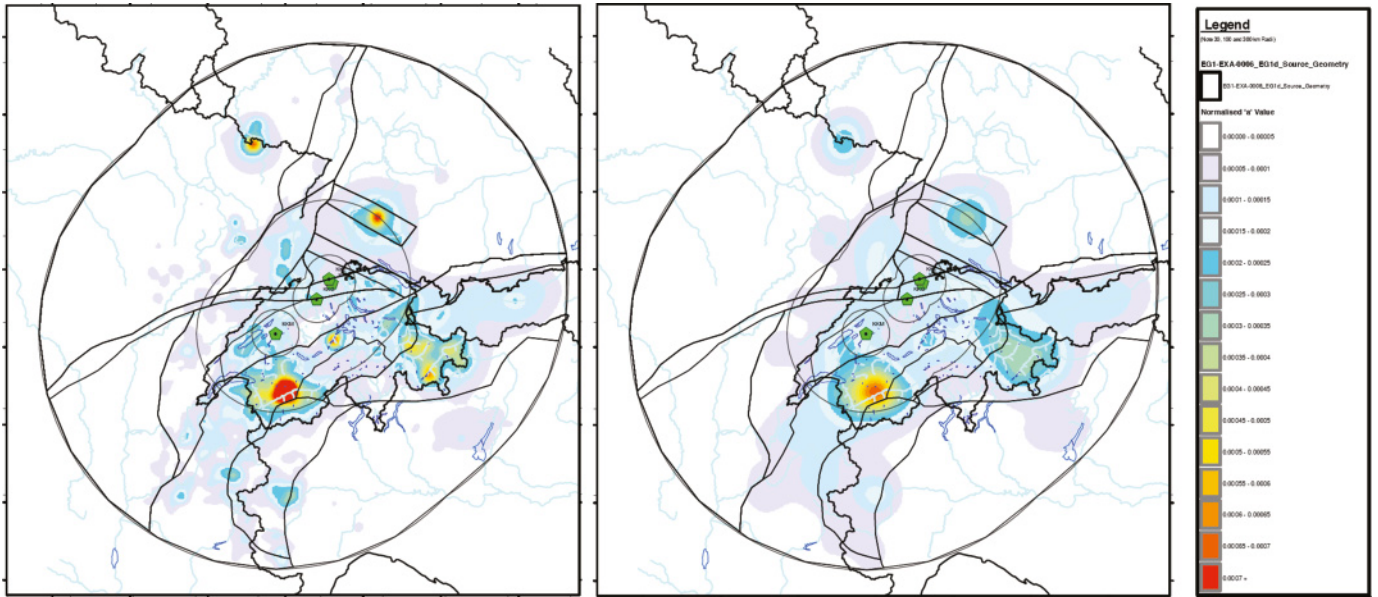


Fig. 5. Map of the study region; color coded is the density of seismicity, smoothed using a kernel of 5 km (left) and 15 km (right). The analysis is based on a Reasenberg declustered catalog, completeness is taken from Ruettener (1995) and applied to the entire region. Note that these figures are the preliminary smoothing masks, which are based on a catalogue that still contains explosion events.

the ECOS catalogue as two sigma bounds, because in our opinion a box distribution makes no sense and was not intended by the SED (Giardini, personal communication, 2002). Thus, the equivalent  $h(\text{error}) = 1/2$  box width.

#### Level 4: Stationarity (boundary properties)

This level again expresses the uncertainty in the degree of stationarity, but also treats the uncertainty in the exact location of boundaries and the idea that seismicity can interact across source zone boundaries. While these three concepts are different and could be expressed separately, we propose that they can all be satisfyingly expressed using a common decision tree level, considering that epicenter uncertainty is also taken into account.

In our model, area source borders can have two properties:

- 1) *Hard*: Rates change abruptly across borders of areal zones. This is based on the assumption that area zone borders are accurate and in essence impermeable for earthquake interaction.
- 2) *Soft*: A soft border allows a gradual transition of rates at zone borders. This is achieved by eroding the rate difference at the border, using a linear gradient with a total width of 5 km. The overall rate (summed activity in both zones) should be conserved in this approach.

The sensitivity feedback establishes that the choice of the boundary properties has only a negligible effect on hazard. We therefore limit our analysis to hard borders.

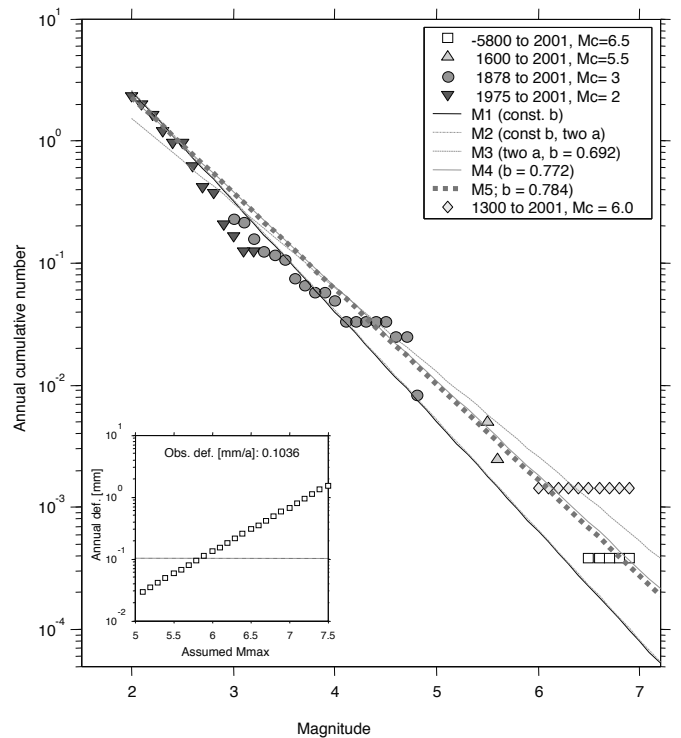


Fig. 6. Left: Sensitivity feedback (hazard). Studied is the 'stationarity' parameter. Low and Medium/High hazard curves are clearly different. Right: Sensitivity of seismic hazard to assumptions regarding magnitude-dependent hypocentral depth: results for 10-Hz PSA.

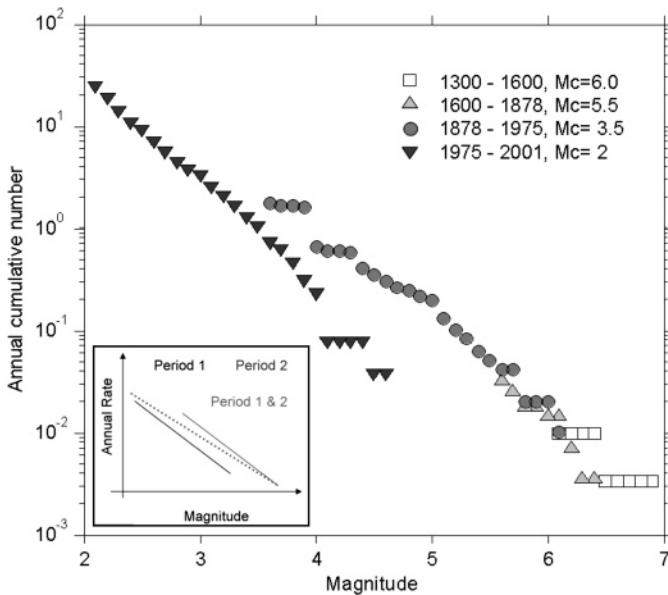


Fig. 7. Annual cumulative number of events as a function of magnitude for earthquakes inside Switzerland and southern Germany for four completeness periods indicated in the legend. Note the offset between the instrumental data (past 1975) and the historical ones. The inset in the lower left shows schematically how the b-value estimation can be systematically biased towards lower values (dashed line) if the rate of activity between two periods is different.

#### Level 5: Completeness

Completeness in magnitude reporting is a critical parameter for rate computation. The magnitude of completeness,  $M_c$ , is defined as the magnitude above which all events are detected for a given period. Its knowledge is needed to accurately compute recurrence parameters (Rydelek & Sacks 1989; Wiemer & Wyss 2000; Wiemer & Wyss 2002). Small changes in the assumed  $M_c$  can produce large changes in b-value and in thus especially in the extrapolated rates of moderate to large main-shocks.  $M_c$  is a complex function of space and time [ $M_c = M_c(x, y, t)$ ], and can only be known with uncertainty (e.g. Wiemer & Wyss 2002). A  $M_c(x, y, t)$  cut much too high, in order to be on the 'safe side', is not a satisfactory solution, because it reduces the amount of available data for rate and b-value estimation, reducing either the spatial resolution or increasing the uncertainty due to the smaller sample sizes (Wiemer & Wyss 2000). An example of the available data for different completeness periods is shown in Figure 7.

$M_c$  needs to be estimated country by country, because differences between national catalogues are the first order boundaries in completeness. The completeness estimate is based on expert judgment, using various plots of the seismicity to appreciate  $M_c$ . The simplest plot of magnitude as a function of time gives a first overview of completeness. We then plot the rate of events for different magnitude bins as a function of time, as well as frequency-magnitude distributions, and identify the major times of changes. This iterative process leads to a definition of completeness periods through time, which is summarized in

table 4. In the case of Switzerland, results are double-checked against estimations of completeness based on the availability of the written historical record (archives) (Faeh et al. 2003). For the instrumental data, completeness is also computed using an algorithm developed for completeness mapping (Wiemer & Wyss 2000).

Completeness estimations, especially for historical data, are only possible with large uncertainties. In order to express the aleatory uncertainty in  $M_c$ , we use two different models of  $M_c(x, y, t)$ . The alternative interpretation (M2) is based on the assumption that historical data are less reliable; hence we assume a higher  $M_c$  for the historical data. Consequently, the alternative model gives relatively less weight to historical data. The sensitivity analysis to recurrence rates (e.g. Fig. 4) confirms that indeed the choice of the completeness model significantly influences the hazard in some zones. We therefore keep both logic tree branches with equal weight in order to express this uncertainty.

#### Level 6: Regional b-value

The regional b-value,  $b_0$  is needed for the subsequent rate determinations for all models (level 9), which allow an overall and constant b-value.  $b_0$  has both aleatory and epistemic uncertainties. The aleatory uncertainty is best computed using bootstrapping of the sample for which  $b_0$  is to be determined, and expressed as a standard deviation,  $\delta b_0$ . This standard deviation is later on also needed for the Bayesian b-value estimation. In addition, there are systematic or model dependent differences for determining  $b_0$ . These different model assumptions are largely based on the fact that the relative weight of instrumental and historical data changes the  $b_0$  estimation considerably. It also takes into account: 1) the possibility that intensities were systematically converted into too high magnitudes, particularly in the period 1880–1970. 2) The possibility that rates changes naturally between different period, which, if completeness changes also, will bias the b-value estimation.

In each model, the b-value is computed using a maximum likelihood fit to a truncated Gutenberg-Richter model (Bender 1983; Utsu 1999), corrected for the magnitude binning (0.1 or 0.5). Completeness varies as a function of space and time, as defined in level 5. The sampled volume for the overall b-value encompasses all events within 300 km from the sites. The four models selected to express the epistemic uncertainty in b-value estimation are:

- 1) **Instrumental b-value only.** This assumes that the b-value obtained from the data between 1975 and 2001 is the most reliable in terms of magnitudes, because it is based on instrumental data rather than macroseismic intensities.
- 2) **Best fit to all data.** This uses all available data (period 1300–2001) above the completeness threshold for computing the overall b-value.
- 3) **Historical only.** By using only the historical data, one avoids mixing two different data sources with different proper-

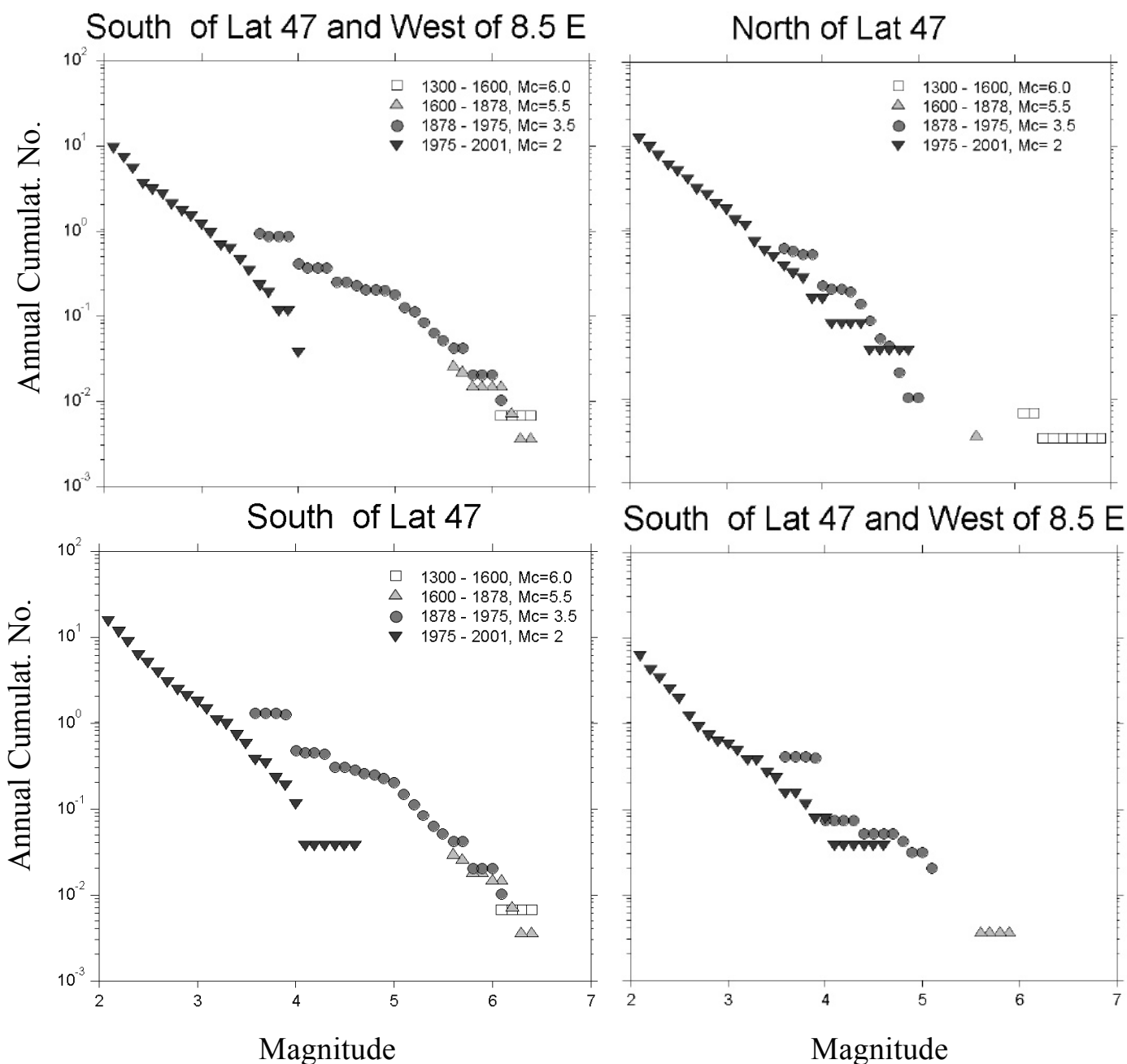


Fig. 8. Same as Figure 7, but for four sub-regions as indicated in the title to each frame. The difference between the instrumental and historical data is most pronounced for the southern and western part of the region (lower left), coinciding with the Valais.

ties. The  $b$ -value computed in this fashion avoids possible biases through mixing these two data sets. The  $b$ -value is computed using a maximum likelihood fit to the data from 1300–1880.

- 4) **Best fit to all data, allowing for a change in the  $a$ -value.** Activity rates in the ECOS catalog vary between historical (particularly the period 1880–1970 and in the Valais area) and instrumental data (Figs. 7 & 8). The observed reduction in the activity rate in the instrumental period

was carefully investigated within PEGASOS (e.g. Fig. 8). It is in our assessment caused by a mixture of natural rate fluctuations, and, possibly, some systematic shift due to the magnitude calibration used in the estimation of macroseismic magnitudes. Because this change in activity coincides with different completeness periods, it causes a systematically biased  $b$ -value (Fig. 7, inset). To avoid this bias, we determine, through a joint maximum likelihood estimation the two rates of seismicity ( $a$ -values) in the

instrumental and historic period, respectively, and one single b-value.

Sensitivity feedback shows that the regional b-value has some, albeit a small effect on the resulting recurrence rates for some zones. We therefore, use all of these aforementioned four models to express the uncertainty on the overall b-value. We have no basis for preferring any one of the models. Accordingly, they are assigned equal weight (0.25).

#### Level 7: Areal zoning

The reasoning for the applied zoning, the justification for each zone and the weights given to these branches are explained earlier on. Our model defines seven decisions to be taken in the areal zoning.

#### Level 8: Mmax determination

The problem of maximum possible magnitude was discussed in previous sections. We capture the epistemic and aleatory uncertainty in Mmax using two equally weighted logic tree branches based on the EPRI approach for extended continental crust, truncated at either M8.0 or M7.5.

#### Level 9: Rate estimation

This final level addresses the epistemic and aleatory uncertainty in rate computation. The basic principles of our rate estimation is 1) Objectivity and reproducibility, hence the rates should be computed in an automatic fashion. 2) Principle of simplicity, hence we will use a simple model with few parameters unless the data require a different approach. To achieve these goals, we develop a multi step scheme to assess the earthquake size distribution (b-value in the Gutenberg-Richter law,  $\log N = a - bM$ , Gutenberg & Richter 1944) and activity rate (a-value). As described when discussing level 5 (overall b-value), assessing rates is complicated through the fact that the activity in certain regions (e.g., the Valais) clearly changes with time.

As a model for representing the frequency and magnitude of events, we use the truncated exponential, which is the earthquake recurrence relationship most commonly used in PSHA (Cornell & Van Marke 1969). It is derived from the Gutenberg & Richter (1944) recurrence model by truncating the rate density of earthquakes at a maximum magnitude,  $m^u$ . The truncated exponential model is given by the expression:

$$N(m) = N(m_0) \frac{e^{-\beta(m-m_0)} - e^{-\beta(m^u-m_0)}}{1 - e^{-\beta(m^u-m_0)}} \quad (1)$$

where  $N(m_0)$  is the annual frequency of earthquakes larger than magnitude  $m_0$ , and  $\beta = b \ln(10)$ . Other recurrence relationships were also considered, but ultimately rejected because there is little evidence for the validity of different recurrence laws in the literature with the exception of the characteristic model.

However, this model is not well suited to the study area because too little is known on the controlling faults.

We use the overall b-value determined in level 6, and then compute the fit of five different models to the observed frequency-magnitude distribution in each zone. The goodness of fit is measure only above the  $M_c(x, y, t)$  cut defined in level 5 for each country. The five models are:

- 1) Constant  $b = b_0$  and variable a-value determined on the entire observation period, taking into account the duration of each completeness period. b is computed using the maximum likelihood method. This model has one free parameter, the a-value.
- 2) Variable  $b$  and  $a$ : Here we determine both the best fitting a- and b-value (in a maximum likelihood sense), hence the model has two free parameters.
- 3) Constant  $b = b_0$  and two variable a-values ( $a_1$  and  $a_2$ ): Here we assume a regional b-value and determine, using a maximum likelihood approach, an a-value for the instrumental data (1975–2000) and one for the historical period (1300–1975). The single, average a-value, used in the predictive PSHA model, is computed as the period weighted average of the two a-values (two free parameters).
- 4) Variable b-value and two variable a-values ( $a_1$  and  $a_2$ ): Here we determine, using a maximum likelihood approach, a b-value a-value for the instrumental data (1975–2000) and one for the historical period (1300–1975). The single average a-value, used in the predictive PSHA model, is computed as the period weighted average of the two a-values (three free parameters).
- 5) Bayesian error weighted b-value: The b-value is determined proportional to the uncertainties and sample sizes of the regional b and the zone-specific b:

$$\text{bayes\_b} = \frac{\text{err0}^2 / (\text{err0}^2 + \text{errb}^2 / N2)}{\text{bwm\_2} + (\text{errb}^2 / N2 / (\text{err0}^2 + \text{errb}^2 / N2)) * b0};$$

where  $\text{err0}$  is the one sigma uncertainty of the overall b-value,  $\text{errb}$  is the one sigma uncertainty of the b-value determined for this particular zone,  $\text{bwm\_2}$  is the b-value determined in model 2,  $b0$  the overall b-value, and  $N2$  the number of samples. The degrees of freedom are then between 1 and 2, computed using the equation:

$$\text{deg\_f} = 1 + (\text{err0}^2 / (\text{err0}^2 + \text{errb}^2 / N2))$$

The fit of each model to the observed data is given as a likelihood,  $L$ . However, because the models have different degrees of freedom (i.e., free parameters), these likelihood scores cannot be directly compared. If two models have the same  $L$ , the one with fewer free parameters should be the preferred model, because a simpler model tends to be more robust. In statistical terms, the decision which model to prefer at each node is based on the Akaike Information Criterion (AIC) score (Imoto 1991; Ogata 1999):

$$\text{AIC}_i = -2 * \ln(L) + 2 * K + (2 * K * (K + 1)) / (n - K - 1)$$

where  $K$  is the number of free parameters, and  $n$  the sample size. The model with the lowest AIC is preferred. This assures that a model with more free parameters (which implies reduced predictability) is only adopted if the data require doing so. For most zones in our model the first model is preferred (const  $b = 0.9$  and variable  $a$ -value). In the Basel zone and in a few other zones, a lower than the regional  $b$ -value is preferred (Model 2).

The AIC score can then be used to obtain weighted alternative models in order to express the epistemic uncertainties in a logical tree approach. The best model is determined by examining their relative distance to the “truth”. The first step is to calculate the difference between model with the lowest AIC and the others as:

$$\Delta_i = \text{AIC}_i - \min \text{AIC}$$

where  $i$  is the difference between the AIC of the best fitting model and that of model  $I$ .  $\text{AIC}_i$  is AIC for model  $i$  and  $\min \text{AIC}$  is the minimum AIC value of all models. The relative weight can be described as:

$$w_i = \frac{\exp(-0.5 * \Delta_i)}{\sum_{r=1}^R \exp(-0.5 * \Delta_r)}$$

where  $w_i$  are known as *Akaike weights* for model  $I$  and the denominator is simply the sum of the relative likelihoods for all candidate models. An example of this kind of computation is shown in Figure 9.

### Treating the uncertainty in magnitude and hypocenter location

Hypocenter locations and magnitudes are uncertain, and these uncertainties are known for each earthquake. In general, uncertainties in location and magnitude for earlier events are larger. Epicenter and magnitude uncertainties are important particularly for large historical events, because a given event could be associated with a number of zones.

In order to incorporate this epistemic uncertainty and quantify its influence on rates and  $b$ -values, we apply a Monte Carlo simulation to levels 8 and 9. In each run of the simulation, a synthetic catalogue is created by randomly shifting each hypocenter and magnitude of individual events. The amount of random shift is based on the probability density function of the uncertainty. The uncertainties in epicentral and magnitude error are based on the ECOS catalog. Having created a randomized catalog, the computation of  $M_{\max}$  and rate in each areal source is repeated. By creating a large number of synthetic catalogs (>100), the uncertainty in  $a$ ,  $b$ - and  $M_{\max}$  based on magnitude and epicenter uncertainty is well resolved.

### Magnitude Dependency of Rupture Depth

The magnitude dependency of rupture depth is one of the factors that might influence site-specific hazard. There is some evi-

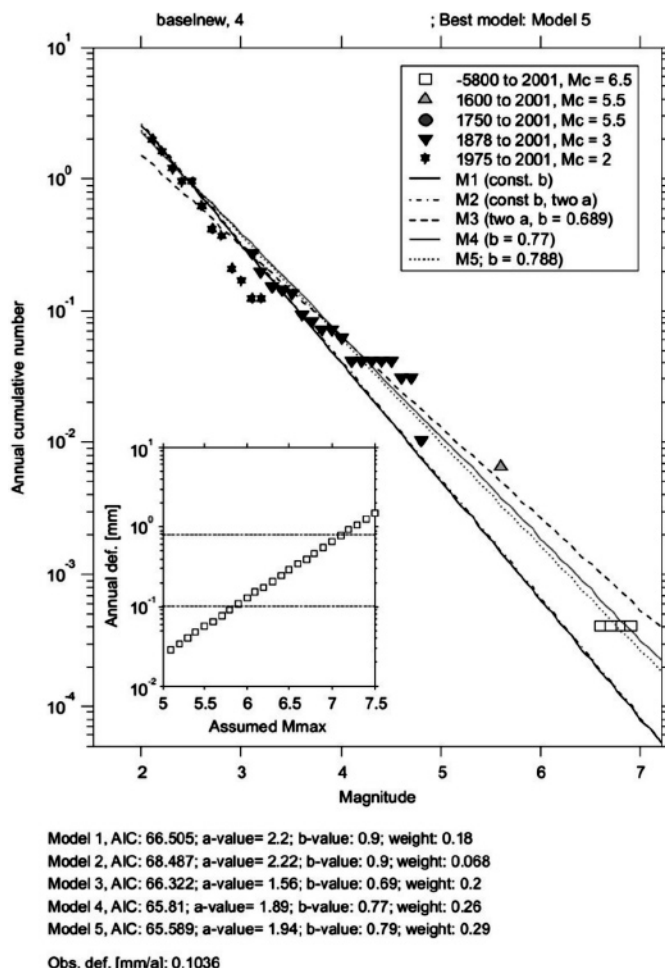


Fig. 9. Cumulative annual rate of events as a function of magnitude for events in the Basel region. Symbols indicate five different completeness periods. The dashed and solid lines show the fit of five different models to the observation, the Akaike Information Criterion (AIC) score of each model is given on the bottom. The small inset displays the annual strain rate in [mm] as a function of assuming  $M_{\max}$ , using a Kostrov (1973) model with a 15 km depth extend of the seismogenic zone. The observed annual deformation from the last 7800 years of observations is about 0.2 mm/yr, when using only the last 700 years, the rate is about 0.8 mm/a.

dence to suggest that the hypocenters of large earthquakes are located in the lower portion of the rupture, and that the aforementioned depth distribution for small events does not apply to large events. In our assessment, there is no specific data for Switzerland or Central Europe that addresses this issue. We therefore must rely on global studies (Wong & Stepp 1998). To assess the influence on our hazard, two models are evaluated: The *Weighted Approach*, which was used in the EPRI (1993) ground-motion study and in the Yucca Mountain study (Wong & Stepp 1998) and an *Un-Weighted Approach*. The sensitivity results show that sensitivity to the treatment of magnitude-dependent hypocentral depths for area sources is very low. This has also implications for the treatment of the Molasse Basin, which we consider not capable of supporting larger ruptures for

lithological/rheological reasons. The magnitude dependence of rupture depth expresses sufficiently our aforementioned opinion that M5+ events cannot originate in the Molasse; therefore, no special treatment of this zone is required. The sensitivity confirms that this is not a critical decision for hazard.

### Earthquake Rupture Geometry

For the hazard computations, it is necessary to define the earthquake rupture geometry. To our knowledge, no specific relationships exist for Switzerland or Central Europe. Therefore, we resort to using globally established relationships. We follow the Wells & Coppersmith (1994) approach for defining the size of earthquake ruptures, using the relationship:

$$\text{Mean } \log_{10}(\text{rupture area}) = 0.91 M - 3.49$$

$$\sigma_{\log_{10}(\text{rupture area})} = 0.24$$

Using the relationship for the expectation of a lognormal distribution, the mean (expected) rupture area is given by the relationship:

$$\text{mean rupture area} = 10^{(0.91 M - 3.424)}$$

The relationship for the mean rupture area will then be used in the hazard computations. The rupture length and width have an aspect ratio of 2.5:1 until the maximum rupture width for a source is reached. The maximum rupture width is determined on the basis of the maximum depth and fault dip, as defined below.

For larger ruptures, the width is held constant at the maximum width and the length is obtained by dividing the rupture area by this width. Earthquake ruptures are located symmetrically with respect to the epicenters, the epicenter being at the midpoint of the rupture. For those epicenters located closer than half the rupture length to the source zone boundary, the ruptures are allowed to extend beyond the source boundary. We use the maximum depths in the distributions (Table 3) as a limit for the ruptures, in order to avoid unrealistically deep ruptures.

The dip angle of ruptures is dependent on faulting style, as defined in Table 2. We assume subvertical dip angles for strike-slip ruptures, 60° dip for normal faulting, and 30° dip for thrusting. These values should be given a standard deviation of plus or minus 20° to remain consistent with the geological information.

### Conclusions

We summarized the process to develop a seismotectonic source model suitable for site-specific hazard assessment at low probability levels, as required in the PEGASOS project (Coppersmith et al. 2008). Exhaustive analysis to identify and quantify epistemic uncertainties associated to the different

parameters and methods involved in the computation procedure, and its treatment through a logic tree approach, have been a key issue of this work. Our seismogenic source model is extensive, with a decision tree of nine levels (Figure 3), which result in 20'160 branches ( $2 * 3 * 3 * 2 * 2 * 4 * 7 * 2 * 5$  decision levels). Because the uncertainties in location and magnitude are captured through a Monte Carlo simulation, the final model contains 100 times more branches. This paper focuses on the rationale we used for decision making, which we hope can be a valuable guide for future projects. However, because of the complexity of the models, we are not able to provide a fully reproducible version (see NAGRA 2004 for more extensive version).

Our seismogenic source model (Eg1d) contains some innovative aspects, specifically related to the assessment of recurrence parameters. The maximum likelihood based approach used in this work was subsequently also employed in deriving the parameters for the Swiss National Hazard maps (Wiemer et al. 2008). We feel that the Akaike weighting is an objective approach to a long-standing question: When should a regional b-value be used, and when a region specific one? We also feel that by using large zones and spatial smoothing within these zones, we are able to represent our conceptual model of the degree of stationarity of seismicity in a reproducible and simple way.

The application of sensitivity feedback from the model parameters provided a useful tool to identify those parameters with a major influence to the final hazard, and allowed to significantly reduce the number of branches in the logic tree. Our experience may offer some guidance on future projects of this kind. In particular, we made the following observations:

- The degree of smoothing (Figure 5) has the strongest effect on the results. Assuming no smoothing produces significantly lower hazard than a Gaussian Kernel of 5 or 15 km.
- The type of declustering played no role in the hazard at the sites, as did the removal of quarry explosions.
- The choice of the regional b-value has a moderate effect; it needs to be represented as a source of uncertainty in the model.
- The estimation of completeness also carries some uncertainty, which can be significant in some zones. This uncertainty is rarely considered in PSHA studies; however, our results suggest that it should be.

### Acknowledgements

This work has benefited from the fruitful interactions with the PEGASOS SP1 TFI team (Kevin Coppersmith and Bob Youngs), and the rest of SP1 Expert Groups. A special memory is devoted to Martin Burkhard, member of EG1b, who passed away in 2006; we dedicate this work to him. We would like to thank the permanent technical and logistic support provided by the staff of Proseis AG, particularly Jim Farrington, René Graf, and Philippe Roth, and the general organizer and project manager Christian Sprecher. We are grateful for the detailed comments of reviewer Stefan Schmid, which greatly helped to improve the clarity of the writing, and for the help of Sabine Woehlbier in producing Figure 2.

## REFERENCES

- Arthaud F. & Matte P. 1975: Les décrochements tardi-hercyniens du Sud-Ouest de l'Europe. *Géométrie et essai de reconstitution des conditions de la déformation. Tectonophysics* 25, 139–171.
- Becker, A., Davenport, C.A. & Giardini, D. 2002: Paleoseismicity studies on end-Pleistocene and Holocene lake deposits around Basle, Switzerland. *Geophysical Journal International* 149, 659–678.
- Bender, B. (1983): Maximum likelihood estimation of b-values for magnitude grouped data. *Bulletin of the Seismological Society of America* 73, 831–851.
- Boyer S. E. & Elliott D. 1982: Thrust systems. *Bulletin of the American Association of Petroleum Geologists* 66(9), 1196–1230.
- Budnitz, R.J., Apostolakis, G., Boore, D.M., Cluff, L.S., Coppersmith, K.J., Cornell, C.A. & Morris, P.A.: Recommendations for PSHA: guidance on uncertainty and use of experts NUREG/CR-6372, vol 1. US Nuclear Regulatory commission, Washington DC, 275 pp.
- Burg J.-P., Van Den Driessche J. & Brun J.-P. 1994: Syn- to post-thickening extension in the Variscan Belt of Western Europe: Mode and structural consequences. *Géologie de la France* 3, 33–51.
- Burkhard M. & Grünthal G. 2009: Seismic source zone characterization for the seismic hazard assessment project PEGASOS by the Expert Group 2 (EG1b). *Swiss Journal of Geosciences* doi: 10.1007/s00015-009-1315-3.
- Burkhard M. 1990: Aspects of the large-scale Miocene deformation in the most external part of the Swiss Alps (Subalpine Molasse to Jura fold belt). *Eclogae Geologicae Helvetiae* 83(3), 559–583.
- Coppersmith K.J., Youngs R.R., Sprecher C. 2009: Methodology and main results of seismic source characterization for the PEGASOS project, Switzerland. *Swiss Journal of Geosciences* doi: 10.1007/s00015-009-1309-1.
- Cornell, C.H., 1968: Engineering seismic risk analysis, *Bulletin of the Seismological Society of America* 58, 1583–1606.
- Cornell, C.A. & Van Marke, E.H. 1969: The Major Influences on Seismic Risk. *Proceedings of the Third World Conference on Earthquake Engineering, Santiago, Chile, Vol. A-1*, 69–93.
- Deichmann, N., Baer, M., Braunmiller, J., allarin Dolfin, D., Bay, F., Delouis, B., Faeh, D., Giardini, D., Kastrup, U., Kind, F., Kradolfer, U., Kuenzle, W., Roethlisberger, S., Schler, T., Salichon, J., Sellami, S., Spuehler, E. & Wiemer, S. 2000: Earthquakes in Switzerland and surrounding regions during 1999, *Physics of The Earth and Planetary Interiors* 93, 395–406.
- Deichmann, N. 1992: Structural and rheological implications of lower crustal earthquakes below northern Switzerland, *Physics of The Earth and Planetary Interiors* 69, 270–280.
- DeMets, C., R.G. Gordon, D.F. Argus, & S. Stein 1990: Current plate motions, *Geophysical Journal International* 101, 425–478.
- Dèzes, P., Schmid, S.M. & Ziegler, P.A. 2004: Evolution of the European Cenozoic Rift System: interaction of the Alpine and Pyrenean orogens with their foreland lithosphere. *Tectonophysics* 389, 1–33.
- Eckardt, P., Funk, H.P. & Labhart, T. 1993: Postglaziale Krustenbewegungen an der Rhein-Rhone-Linie. *Vermessung, Photogrammetrie, Kulturtechnik* 2, 43–56.
- Electric Power Research Institute (EPRI) 1993: Guidelines for Determining Design Basis Ground Motions, Early Site Permit Demonstration Program, Vol.1, RP3302, Electric Power Res. Inst., Palo Alto, California.
- Fäh, D., Giardini, D., Bay, F., Bernardi, F., Braunmiller, J., Deichmann, N., Furrer, M., Gantner, L., Gisler, M., Isenegger, D., Jiménez, M.J., Kästli, P., Koglin, R., Masciadri, V., Rutz, M., Scheidegger, C., Schibler, R., Schorlemmer, Schwarz-Zanetti, G., Steimen, S., Sellami, S., Wiemer, S. & Wössner, J. 2003: Earthquake Catalogue Of Switzerland (ECOS) and the related macroseismic database. *Eclogae Geologicae Helvetiae* 96(2), 219–236.
- Frankel, A., Mueller C., Barnhard T., Perkins D., Leyendecker E.V., Dickman N. Hanson, S. & Hopper. M. 1997: Seismic hazard maps for California, Nevada and western Arizona/Utah, United States Geological Survey Open-File Report, 97–130.
- Frankel, A. 1995: Mapping seismic hazard in the central and eastern United States, *Seismological Research Letters* 66, 8–21.
- Gardner, J.K. & Knopoff, L. 1974: Is the sequence of earthquakes in Southern California, with aftershocks removed, Poissonian? *Bulletin of the Seismological Society of America* 64, 1363–1367.
- Grellet B., Combes Ph., Granier Th., Philip H. & Mohammadioun B. 1993: Sismotectonique de la France métropolitaine dans son cadre géologique et géophysique, avec atlas de 23 cartes au 1/4'000'000 et une carte au 1/1'000'000. *Mémoire de la Société Géologique de France* 64(1) 76 pp., 64(2), 24 pl. et 1 carte.
- Giardini, D. 1999: The Global Seismic Hazard Assessment Program (GSHAP) – 1992/1999, *Annali de Geofisica* 42, 957–974.
- Gutenberg, R., & Richter, C.F. 1944: Frequency of earthquakes in California, *Bulletin of the Seismological Society of America* 34, 185–188.
- Homberg, C., Angelier J., Bergerat F. & Lacombe O. 1994: New Tectonic Data in the External Jura – Contribution of Paleostress Reconstructions, *Comptes rendus de l'Académie des sciences. Série 2. Sciences de la terre et des planètes* 318(10), 1371–1377.
- Homberg, C., Hu J.C., Angelier J., Bergerat F. & Lacombe O. 1997: Characterization of stress perturbations near major fault zones: Insights from 2-D distinct-element numerical modelling and field studies (Jura mountains). *Journal of Structural Geology* 19(5), 703–718.
- Hsü K.J. 1995: The geology of Switzerland: An introduction to tectonic facies. Princeton University Press, Princeton, New Jersey, USA, 250 pp.
- Husen S., Kissling E., Deichmann N., Wiemer, S., Giardini D. & Baer M. 2003: Probabilistic earthquake location in complex three-dimensional velocity models: Application to Switzerland. *Journal of Geophysical Research* 108 (B2), 2003.
- Imoto, M. 1991: Changes in the Magnitude Frequency b-Value Prior to Large (M- Greater-Than-or-Equal-to-6.0) Earthquakes in Japan, *Tectonophysics* 193(4), 311–325.
- Jaboyedoff, M. & Pastorelli, S. 2003: Perturbation of the heat flow by water circulation in a mountainous framework: Examples from the Swiss Alps, *Eclogae geologicae Helvetiae* 96, 37–47.
- Johnston, A.C., Coppersmith K.J., Kanter L.R., & Cornell C.A. 1994: The Earthquakes of Stable Continental Regions: Vol. 1: Assessment of Large Earthquake Potential. Electric Power Research Institute (EPRI TR-102261-V1).
- Kagan, Y., & D. Jackson 2000: Probabilistic forecasting of earthquakes. *Geophysical Journal International* 143, 438–453.
- Kagan, Y. 1999: Universality of the seismic moment-frequency relation. *Pure and Applied Geophysics* 155, 537–574.
- Kastrup, U., Deichmann, N., Fröhlich, A. & Giardini, D. 2007: Evidence for an active fault below the northwestern Alpine foreland of Switzerland. *Geophysical Journal International* 169, 1273–1288.
- Kijko, A., & Graham G. 1998: Parametric-historic procedure for probabilistic seismic hazard analysis – Part I: Estimation of maximum regional magnitude Mmax. *Pure and Applied Geophysics* 152(3), 413–442.
- Kijko, A., Lasocki S & Graham G. 2001: Non-parametric Seismic Hazard in Mines, *Pure and Applied Geophysics* 158(9–10), 1655–1675, 2001.
- Kissling, E. 1993: Deep-Structure of the Alps – What Do We Really Know. *Physics of the Earth and Planetary Interiors* 79(1–2), 87–112.
- Kostrov, B.V. 1974: Seismic moment and energy of earthquakes and seismic flow of rock., *Izvestiya, Academy of Sciences, USSR, Physics of the Solid Earth* 1, 23–44.
- Mancktelow N. 1985: The Simplon Line: a major displacement zone in the Western Lepontine Alps. *Eclogae geologicae Helvetiae* 78, 73–96.
- Meghraoui, M., Delouis, B., Ferry, M., Giardini, D., Huggenberger, P., Spotte, I. & Granet, M. 2001: Active normal faulting in the Upper Rhine Graben and paleoseismic identification of the 1356 Basel earthquake. *Science* 293, 2070–2073.
- Musson, R., Sellami, S. & Brüstle, W. 2009: Preparing a seismic hazard model for Switzerland: The view from PEGASOS Expert Group 3 (EG1c). *Swiss Journal of Geosciences* doi: 10.1007/s00015-008-1301-1.
- Muttoni, G., Garzanti, E., Alfonsi, L., Cirilli, S., Germani, D., & Lowrie, W. 2001: Motion of Africa and Adria since the Permian: paleomagnetic and paleoclimatic constraints from northern Libya. *Earth and Planetary Science Letters* 192(2), 159–174.
- NAGRA 2004: Probabilistic Seismic Hazard Analysis for Swiss Nuclear Power Plant Sites (PEGASOS Project) prepared for Unterausschuss Kernener-

- gie der Überlandwerke (UAK). Final Report Vol. 1–6, 2557 pp. To be obtained on request at swissnuclear by writing to info@swissnuclear.ch.
- Niviere, B., & Winter T. (2000): Pleistocene northwards fold propagation of the Jura within the southern Upper Rhine Graben: seismotectonic implications. *Global and Planetary Change* 27(1–4), 263–288.
- Ogata, Y. 1999: Seismicity analysis through point-process modeling: A review. *Pure and Applied Geophysics* 155(2–4), 471–507.
- Pavoni N., Maurer H.R., Roth P. & Deichmann N. 1997: Seismicity and seismotectonics of the Swiss Alps, In: Pfiffner et al. (Eds.): *Deep Structure of the Swiss Alps*. Results of NRP 20. Birkhäuser Verlag, Basel.
- Regenauer-Lieb, K. & Petit J.P. 1997: Cutting of the European continental lithosphere: Plasticity theory applied to the present Alpine collision. *Journal of Geophysical Research* 102(B4), 7731–7746.
- Ricou L.E. 1994: Tethys reconstructed: plates, continental fragments and their boundaries since 260 Ma from Central America to South-eastern Asia. *Geodinamica Acta* 7(4), 169–218.
- Rydelek, P.A. & Sacks I.S. 1989: Testing the completeness of earthquake catalogs and the hypothesis of self-similarity, *Nature* 337, 251–253.
- Schmid S. M. & Slejko D. 2009: Seismic source characterization of the Alpine foreland in the context of a probabilistic seismic hazard analysis by PEGASOS Expert Group 1 (EG1a). *Swiss Journal of Geosciences* doi: 10.1007/s00015-008-1300-2.
- Schmid S.M. & Kissling E. 2000: The arc of the western Alps in the light of geophysical data on deep crustal structure. *Tectonics* 19(1), 62–88.
- Schmid, S.M., Froitzheim N., Pfiffner O.A., Schonborn G. & Kissling E. 1997: Geophysical-geological transect and tectonic evolution of the Swiss-Italian Alps. *Tectonics* 16(1), 186–188.
- Schumacher, M.E. 2002: Upper Rhine Graben: Role of preexisting structures during rift evolution, *Tectonics*, 21, 1006, doi:10.1029/2001TC900022
- Sissingh, W. 1998: Comparative Tertiary stratigraphy of the Rhine Graben, Bresse Graben and Molasse Basin: correlation of Alpine foreland events. *Tectonophysics* 300(1–4), 249–284.
- Sissingh W. 2001: Tectonostratigraphy of the West Alpine Foreland: correlation of Tertiary sedimentary sequences, changes in eustatic sea-level and stress regimes. *Tectonophysics* 333, 361–400.
- Slejko, D. Peruzza, L. & Rebez, A. 1998: Seismic hazard maps of Italy. *Annali di Geofisica* 41 (2), 183–214.
- Sommaruga A. 1999: Décollement tectonics in the Jura foreland fold-and-thrust belt. *Marine and Petroleum Geology* 16, 111–134.
- Truffert C., Burg J.-P., Cazes M., Bayer R., Damotte B. & Rey D. 1990: Structures crustales sous le Jura et la Bresse: contraintes sismiques et gravimétriques le long des profils ECORS Bresse-Jura et Alpes II. *Mémoires de la Société Géologique de France* 156, 157–164.
- Trümpy R. 1985: Die Plattentektonik und die Entstehung der Alpen. *Neujahrsblatt der Naturforschenden Gesellschaft Zürich*, Heft Nr. 187, 45 pp.
- Utsu, T. 1999: Representation and analysis of the earthquake size distribution: A historical review and some new approaches. *Pure and Applied Geophysics* 155, 509–535.
- Veneziano, D., Cornell C.A. & O'Hara R. 1984: Historical method of seismic hazard analysis, Technical Report NP-3438, Electric Power Research Institute, Palo Alto, California, 178 pp.
- Villemin, T., Alvarez F. & Angelier J. 1986: The Rhinegraben – Extension, Subsidence and Shoulder Uplift. *Tectonophysics* 128(1–2), 47–59.
- Wells, D.L., & Coppersmith K.J. 1994: New Empirical Relationships among Magnitude, Rupture Length, Rupture Width, Rupture Area, and Surface Displacement. *Bulletin of the Seismological Society of America*, 84(4), 974–1002.
- Wiemer S. & Wyss M. 2002: Mapping spatial variability of the frequency-magnitude distribution of earthquakes. *Advances in Geophysics* 45, 259–302.
- Wiemer, S. & Baer M. 2000: Mapping and removing quarry blast events from seismicity catalogs. *Bulletin of the Seismological Society of America* 90, 525–530.
- Wiemer, S. & Wyss M. 2000: Minimum magnitude of complete reporting in earthquake catalogs: examples from Alaska, the Western United States, and Japan. *Bulletin of the Seismological Society of America* 90, 859–869.
- Wiemer, S., Giardini, D., Fäh, D., Deichmann N. & Sellami S. 2008: Probabilistic Seismic Hazard Assessment of Switzerland: Best Estimates and Uncertainties. *Journal of Seismology*, doi: 10.1007/s10950-008-9138-7.
- Wong, I.G. & Stepp, C. 1998: Probabilistic seismic hazard analyses for fault displacement and vibratory ground motion at Yucca Mountain, Nevada. DE-AC04-94AL8500, for U.S. Geological Survey and U.S. Department of Energy, by Civilian Radioactive Waste Management System, Management and Operating Contractor, Oakland, CA, Vol. 1: Text, 645 pp.; Vol. 2: Appendices A–E; Vol. 3: Elicitation Summaries, Appendices F–J.
- Woo, G. 1996: Kernel estimation methods for seismic hazard area source modeling. *Bulletin Seismological Society of America* 86(2), 353–362.
- Ye, S., Ansonge J., Kissling E. & Mueller S. 1995: Crustal Structure beneath the Eastern Swiss Alps Derived from Seismic-Refraction Data, *Tectonophysics* 242(3–4), 199–221.
- Ziegler P. A. 1992: European Cenozoic rift system. *Tectonophysics* 208, 91–111.

Manuscript received August 4, 2008

Revision accepted Oktober 10, 2008

Published Online first March 28, 2009

Editorial Handling: Stefan Bucher